ORNL-5660

ornl

OAK RIDGE NATIONAL LABORATORY

UNION CARBIDE

Mechanical Properties of 16-8-2 Large-Diameter Pipe Girth Welds

R. L. Klueh
D. P. Edmonds

METALS and CERAMICS
ENERGY
RESEARCH
DEVELOPMENT
OAK RIDGE NATIONAL LABORATORY

OPERATED BY
UNION CARBIDE CORPORATION
FOR THE UNITED STATES
DEPARTMENT OF ENERGY

ORNL-5660
Distribution
Categories
UC-79h, -k, -r

Contract No. W-7405-eng-26

METALS AND CERAMICS DIVISION

MECHANICAL PROPERTIES OF 16-8-2 LARGE-DIAMETER PIPE GIRTH WELDS

R. L. Klueh and D. P. Edmonds

Date Published: September 1980

OAK RIDGE NATIONAL LABORATORY
Oak Ridge, Tennessee 37830
operated by
UNION CARBIDE CORPORATION
for the
DEPARTMENT OF ENERGY

CONTENTS

MECHANICAL PROPERTIES OF 16-8-2 LARGE-DIAMETER PIPE GIRTH WELDS*

R. L. Klueh and D. P. Edmonds

ABSTRACT

The 16-8-2 weld filler metal is used extensively to weld type 316 stainless steel. We determined the elevated-temperature mechanical properties of 16-8-2 weld metal specimens taken from girth welds that were made by the automatic gas tungsten-arc process on 0.71-m-diam type 316 stainless steel seamless pipe with a 9.5-mm-thick wall. For comparison the properties of the type 316 stainless steel pipe were also determined at three pipe positions relative to the weld: at a position adjacent to the weld (the heat-affected zone), at a position of maximum residual stress caused by welding, and at a large distance from the weld.

Over the range 25 to 649°C the yield strength of the 16-8-2 weld metal exceeds the strength of the pipe both in the heat-affected zone and at a large distance from the weld. The yield strength of the pipe at the position of maximum residual stress from welding was similar to that of the 16-8-2 weld metal. Except at room temperature the ultimate tensile strength of the 16-8-2 weld metal (up to 649°C) is considerably less than that of the type 316 stainless steel pipe. At room temperature their properties essentially do not differ. Furthermore, the ultimate tensile strength of the type 316 stainless steel pipe taken from different positions in the pipe does not differ.

The creep-rupture properties were determined at 566 and 649°C. The strength of the 16-8-2 weld metal was below that of the type 316 stainless steel pipe. However, there were indications that the strength of the weld metal approached the strength of the type 316 stainless steel pipe at long rupture times. This approach of properties was even more evident when the stress-minimum creep rate relationships were compared. The differences in the creep behavior of the 16-8-2 and type 316 stainless steel were explained by the metallurgical processes that occur in these stainless steels.

---

*Work performed under DOE/RRT AF 15 10 15, Task OR-1.3, Mechanical Properties Design Data.

INTRODUCTION

Weldments very often are critical structural elements in nuclear systems. The Fast-Flux Test Facility (FFTF) contains several critical welds throughout the primary vessel. Included in these welds are several large-diameter pipe welds that will operate in the temperature range where deformation can occur by creep, 450 to 550°C. The hot-leg piping is type 316 stainless steel joined with 16-8-2 weld metal. Our primary objective was to determine the elevated-temperature properties of pipe welds that are prototypic of the FFTF pipe welds. With such data the designer will be better able to evaluate the expected performance of these welds in the operating reactor.

EXPERIMENTAL

We obtained six prototypic FFTF 16-8-2 spoolpiece girth welds made on 0.71-m-diam type 316 stainless steel seamless pipe with a 9.5-mm-thick wall. The welds were made by HUICO, Inc., Richland, Washington, using the same welding procedures and inspection techniques that they used to weld the primary loop piping for the FFTF hot leg. The 16-8-2 filler wire and type 316 stainless steel seamless pipe were from the same stock as that used for FFTF construction. The chemical composition of the material is shown in Table 1, and the mechanical properties are shown in Table 2.

Pipe lengths of 0.35 m were joined with a single-vee joint by the automatic gas tungsten-arc process with cold-wire filler additions in the 1-G position (the pipe was rotated beneath the torch). These pipe sections were longer than the minimum required to model infinite pipe lengths, that is, the effect of pipe length on stress in the weldment was negligible. Eight fill passes were used on the joint. An etched cross section of the pipe weld is shown in Fig. 1.

Table 1. Chemical Composition of Type 316 Stainless Steel Pipe and 16-8-2 Filler Wire and Weld

Element	Content, wt %				
	16-8-2 Weld			Type 316 Stainless Steel (Heat 55318)	
	Weld Wire[a]	Weld[b]			
		Top	Bottom	Vendor[c]	ORNL
C	0.045	0.051	0.051	0.055	0.067
Mn	1.25	1.42	1.37	1.78	1.96
Si	0.29	0.33	0.33	0.38	0.36
S	0.01	0.011	0.012	0.012	0.012
P	0.02	0.032	0.026	0.022	0.020
Cr	16.36	15.97	15.93	16.45	16.52
Ni	8.62	9.76	9.89	13.52	13.36
Mo	1.67	1.73	2.07	2.16	2.17

[a]Vendor: Arcos Corporation, Philadelphia.

[b]ORNL analysis.

[c]Vendor: Cameron Iron Works, Inc., Houston, Texas.

Table 2. Mechanical Properties of Type 316 Stainless Steel Pipe and 16-8-2 Filler Wire as Reported by Vendors

Property	16-8-2 Weld Wire[a]	Type 316 Stainless Steel[b] (Heat 55318)
Yield strength, MPa	362	283
Tensile strength, MPa	604	567
Elongation, %	47	53.7
Reduction of area, %	70	69.3
Ferrite number	2	

[a]Vendor: Arcos Corporation, Philadelphia.

[b]Vendor: Cameron Iron Works, Inc., Houston, Texas.

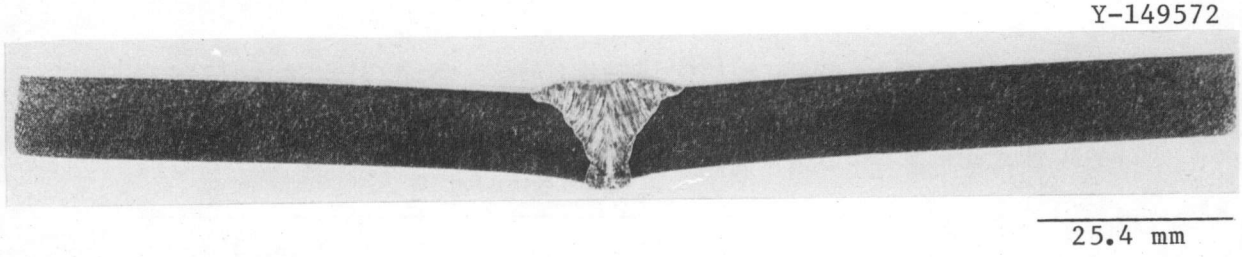

Fig. 1. Cross Section of 16-8-2 Pipe Weld.

The δ-ferrite content of the weld was determined with a Ferrite Scope. After eight readings an average ferrite number (FN) of 2.5 was determined for the weld crown with little variation across the surface. From crown to root the FN decreased from 2.5 to 0.7. The FN also decreased as the weld metal-base metal interface was approached; the FN of the type 316 stainless steel pipe was essentially zero (<0.1).

The difference in FN and ferrite morphology (Fig. 2) going from the crown to root probably results from the higher dilution at the root. The microstructure of the type 316 stainless steel pipe was typical of such a product form (Fig. 3). The microstructure varied little with pipe position: similar microstructures were observed adjacent to the weld [the heat-affected zone (HAZ)], 64 mm from the weld centerline, and at a position well removed from the weld (0.28 m from the weld).

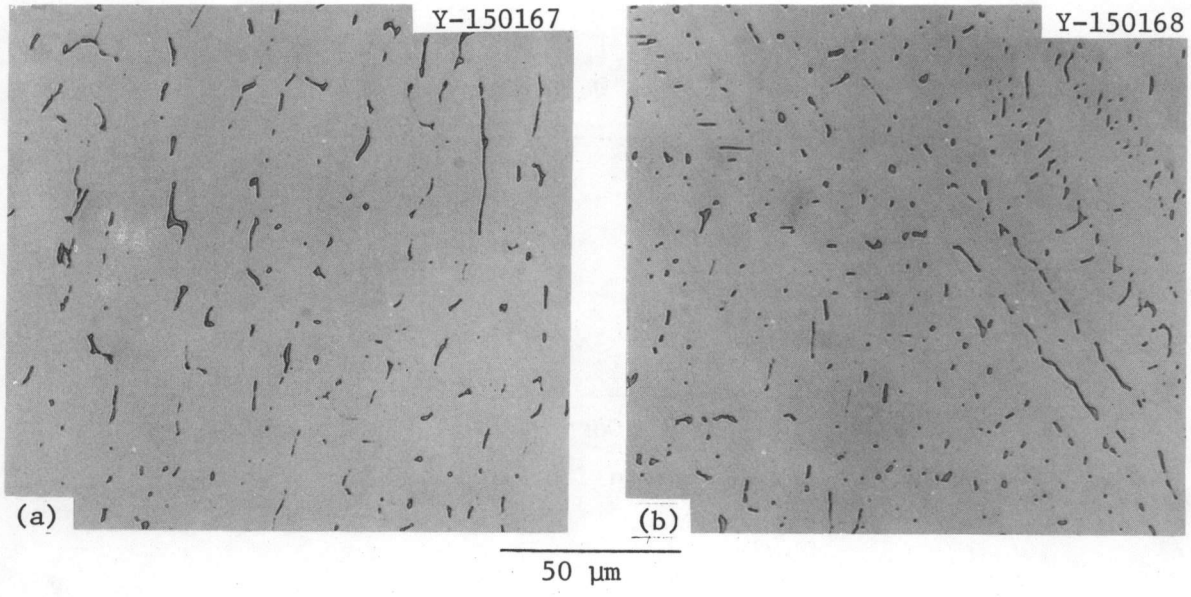

Fig. 2. Microstructure of 16-8-2 Pipe Weld at (a) Root and (b) Center of the Weld.

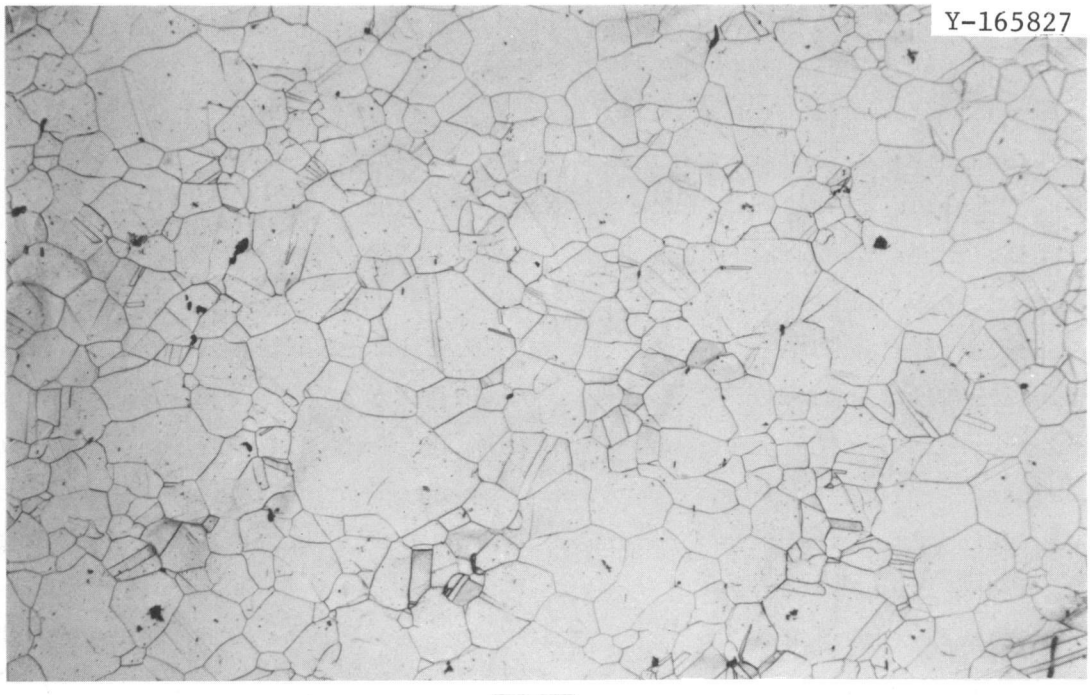

Fig. 3. Microstructure of the Type 316 Stainless Steel Pipe.

Longitudinal and transverse test specimens were taken from the welds. The longitudinal specimens contained only 16-8-2 weld metal in the gage length, while the transverse specimens contained weld metal in the center third of the gage length. The remainder was base metal. Since the amount of weld metal was limited and because of the limited thickness of the pipe, specimens were fabricated by machining 57.15-mm-long blanks, 7.93 mm in diameter from the longitudinal and transverse directions. These blanks were then welded to 19.0-mm-diam type 316 stainless steel end pieces with a low heat input. From these blanks our standard tensile specimens were machined. These specimens had a 6.35-mm-diam by 31.70-mm-long reduced section.

Type 316 stainless steel base metal specimens were taken from three positions in the pipe: from immediately adjacent to the weld (HAZ), from about 64 mm from the weld centerline, and from about 0.28 m from the weld centerline. All specimens were taken tangentially, that is, the specimens

were machined parallel to the pipe weld. The 64-mm position was chosen because ultrasonic wave studies showed this as the position of maximum residual stress in the pipe from welding.[1] The specimens 0.28 m from the weld should be representative of pipe that was unaffected by welding.

Tensile tests were made at 2.67×10^{-6} and 6.67×10^{-5} s nominal strain rates over the range 25 to 649°C. Fewer transverse specimens were tested than longitudinal specimens. Tests were made in air on a 44-kN Instron test machine. Specimens were heated in a three-zone resistance furnace with temperature controlled to ±1°C with less than a 2°C temperature variation along the specimen gage length. The Instron test machine was operated at a constant crosshead velocity, and the strain rate was determined from the crosshead velocity and the initial gage length.

The creep-rupture tests were made in air at 566 and 649°C on lever-arm creep frames with 10 to 1 ratios; the specimens were heated with Marshall resistance furnaces. During test the temperature was monitored and controlled by three Chromel-vs-Alumel thermocouples attached along the specimen gage section. Creep strains were measured with a mechanical extensometer attached to the specimen shoulders, and the strain was read periodically on a dial gage with a sensitivity of 0.3 μm.

RESULTS

Tensile Properties

Tensile properties were determined over the range 25 to 649°C for the 16-8-2 longitudinal and transverse weldment specimens (Table 3) and for type 316 stainless steel pipe (Table 4). Most tests were made at a strain rate of 6.67×10^{-5}/s with a few tests at 2.67×10^{-6}/s.

Longitudinal weld metal specimens were tested from two pipe welds. There was little or no difference in yield strength (YS) and ultimate tensile strength (UTS) of the two welds (Fig. 4).

The base metal properties of the type 316 stainless steel pipe were determined from specimens taken from three different positions: immediately adjacent to the weld (HAZ), approximately 64 mm from the weld centerline, and about 0.28 m from the weld (Table 4). In Fig. 4 the base metal YS and UTS are compared with the weld metal properties.

Table 3. Tensile Properties of 16-8-2 Pipe Welds

Weld	Temperature	Strength, MPa			Elongation, %		Reduction of Area (%)
		0.2% Yield	Ultimate Tensile	Fracture	Uniform	Total	
			Longitudinal Specimens[a]				
1[b]	25	355	590	422	50.4	63.1	76.6
	204	258	452	314	27.4	42.7	67.9
	316	248	471	363	32.2	42.6	57.1
	427	230	452	244	31.8	49.2	49.2
	566	226	387	168	27.4	40.0	60.1
	649	198	264	103	16.4	54.7	67.2
2[b]	25	347	605	146	57.7	64.4	72.7
	204	268	457	328	28.8	36.3	67.1
	316	248	459	347	28.2	53.3	55.7
	454	218	450	373	35.0	39.8	38.7
	510	220	429	343	30.0	35.8	52.1
	566	210	381	277	26.0	34.1	76.0
	649	208	367	142	11.4	43.0	69.0
2[c]	25	321	579	475	54.4	62.9	69.7
	454	233	468	407	30.5	37.0	53.3
	566	215	288	139	19.8	49.6	71.9
	649	199	218	102	4.0	35.0	69.9
			Transverse Specimens[d]				
1[b]	25[e]	349	621	377	43.2	64.6	78.2
	566	190	405	168	18.4	26.0	57.3
	649	204	307	182	19.8	20.6	56.6
2[b]	25[e]	315	615	375	48.8	60.2	77.5
	204	236	557	405	25.6	30.4	56.2
	454	189	488	415	28.3	32.1	59.1
	566	193	424	364	20.0	23.2	53.2
	649	176	208	219	12.1	18.5	57.3

[a]All-weld-metal specimens.

[b]Tested at a strain rate of 6.67×10^{-5}/s.

[c]Tested at a strain rate of 2.67×10^{-6}/s.

[d]Gage length contained weld metal only in center (no more than one-fourth of the gage length contained weld metal).

[e]Failed in base metal, although there was considerable deformation in weld metal. All other transverse specimens failed in weld metal with essentially no deformation in base metal.

Table 4. Tensile Properties of Type 316 Stainless Steel

Strain Rate (s^{-1})	Temperature (°C)	Strength, MPa		Elongation, %		Reduction of Area (%)
		Yield	Ultimate	Uniform	Total	
	Adjacent to Weld (Heat-Affected Zone)					
6.67×10^{-5}	25	248	601	56.1	65.7	64.6
	204	162	500	42.6	51.2	51.1
	316	147	532	48.2	54.3	54.7
	427	135	515	57.2	57.7	58.2
	566	121	457	50.6	57.6	53.5
	649	119	308	35.9	64.2	63.8
6.67×10^{-5}[a]	25	258	584	58.1	69.4	64.3
	204	177	507	44.0	49.0	56.1
	316	160	519	47.6	52.6	54.2
	454	144	502	49.9	54.0	55.7
	510	138	493	51.8	56.6	54.6
	566	130	441	43.2	54.6	53.5
	649	128	335	37.2	65.0	62.0
2.67×10^{-6}	25	246	572	54.8	70.2	67.1
	566	129	408	30.0	43.4	39.3
	649	126	255	21.6	56.0	65.7
	64 mm from Weld Centerline					
6.67×10^{-5}	25	352	612	45.7	59.8	64.0
	204	236	514	37.2	45.9	57.0
	316	246	530	38.1	43.8	51.3
	427	213	526	41.8	50.0	55.3
	566	212	460	39.7	48.0	51.0
	649	186	333	29.0	59.2	61.4
	0.28 m from Weld					
6.67×10^{-5}	25	251	592	56.3	67.0	68.0
	482	133	502	57.1	52.3	52.4
	566	126	464	45.0	52.5	53.0
	649	120	335	37.6	65.8	60.3

[a]This series of tests was from pipe 2; all other tests were on pipe 1.

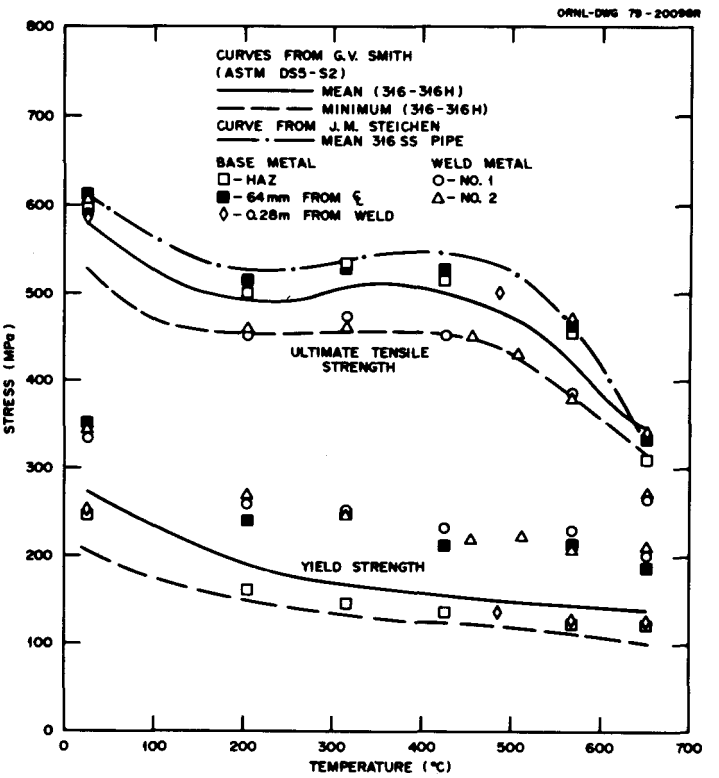

Fig. 4. Yield Strength and Ultimate Tensile Strength as Functions of Temperature for 16-8-2 Pipe Welds and Type 316 Stainless Steel Pipe. Curves for average and minimum properties for type 316 stainless steel are also shown.

Specimens were taken 64 mm from the weld because this position was found to be the point of maximum residual stress.[1] As seen in Fig. 4 the YS of base metal from this position is higher than that of the base metal of the other two positions. However, the UTS for base metal from the three different positions essentially does not differ.

At all temperatures the YS of the 16-8-2 weld metal is considerably greater than that for the type 316 stainless steel base metal from the HAZ and from 0.28 m from the weld. The YS values of base metal from these two positions do not differ. However, the YS of the base metal at the position of maximum residual stress is comparable to or slightly less than that of the weld metal.

For comparison average and minimum trend curves for the YS and UTS of type 316 stainless steel are also shown in Fig. 4. These were taken from the data compilation of Smith.[2] The YS of the 16-8-2 weld metal falls well above Smith's average value, while the UTS falls well below the average — very near the minimum. The YS values of the type 316 stainless steel pipe taken 64 mm from the weld centerline were similar to those for the weld metal. The YS values from the other positions were below the mean but above the minimum. The UTS values for the base metal, which showed no difference from one position to another, were above Smith's average.

Steichen[3] tested type 316 stainless steel pipe similar to that tested in this study. The mean UTS curve from his report is also shown in Fig. 4. The base metal properties determined in this study agree quite well with Steichen's results. Steichen's YS values were similar to or just slightly less than the Smith average. Yield strength values from this study were slightly less (about 10%) than Steichen's values.[3]

Based on the observed deformation and fracture characteristics of the transverse weldment specimens, the YS and UTS values of these specimens were in general agreement with the base metal and longitudinal weld metal tests (Table 3). Since the transverse specimens contain weld metal in only a small portion of the gage section, we would not necessarily expect the two types of specimens to have similar strengths. The transverse specimens tested at 25°C fractured in the base metal, although the weld metal appeared to have a neck. The transverse specimens tested at all other temperatures failed in the center of the weld metal with only a small amount of deformation occurring in the base metal (there was only about a 10% reduction of area in the base metal). As seen in Fig. 4, at 25°C the UTS of the longitudinal weld metal specimens is similar to that for the base metal; thus, the failure in the base metal at 25°C is not unexpected. At most of the other temperatures the strength properties of the transverse weldment specimens fall midway between the weld metal and the base metal (Table 3).

The ductility values for the weld metal and base metal show no large differences (Fig. 5). Total elongation and reduction of area values are quite large for all tests. The uniform elongation values of the longitudinal weld metal specimens fall off at elevated temperatures more than the decrease noted for any of the type 316 stainless steel base metal.

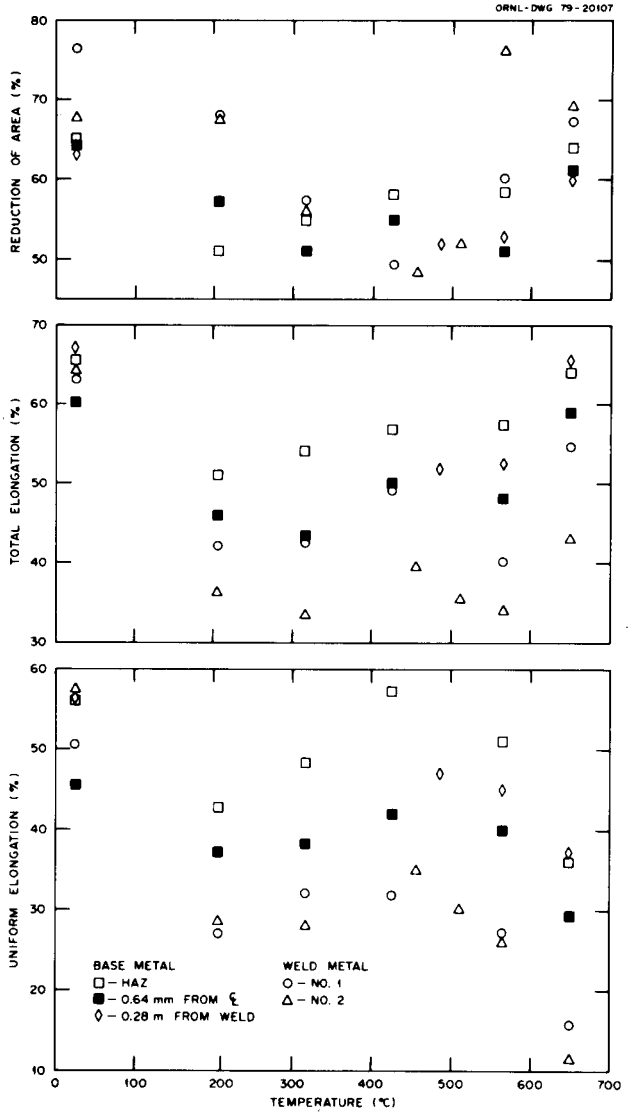

Fig. 5. Uniform Elongation, Total Elongation, and Reduction of Area as Functions of Temperature for 16-8-2 Pipe Welds (Longitudinal Weld Specimens) and Type 316 Stainless Steel Pipe from Three Positions in the Pipe.

The elongation measurements for the transverse and longitudinal specimens are not directly related (Table 3). The elongations for both types of specimens were calculated for the entire gage length. However, as stated above, except for the transverse specimens tested at 25°C, deformation was almost entirely in the weld metal, which made up only part of the gage section. Therefore, the actual gage length over which the true total elongation should be calculated is unknown but is much less than the total gage length.

Strain rate had the expected effect. The properties were affected minimally except at the highest test temperatures, where the UTS was considerably decreased for the lower strain rate tests. This occurs for both the weld metal and the base metal. The decrease in UTS is accompanied by a decrease in uniform elongation.

Visual observations on fractured specimens revealed that the failures were all ductile, either cup-cone or ductile shear types. This was true for the 16-8-2 longitudinal and transverse weld specimens and for the type 316 stainless steel, regardless of the position in the pipe from which it was removed.

The weld metal specimens exhibited anisotropic deformation characteristics. Generally, the deformed cross section was an ellipse rather than a circle. The other anisotropic deformation appeared "knobby," as if various regions along the gage length were in the process of necking — in addition to the region that necked to failure. Metallographic examination of selected weld metal specimens revealed only ductile fractures. The anisotropic deformation termed "knobby deformation" was attributed to microstructural features (differences in substructural orientations within neighboring grains), as has previously been observed for weld metals.[4,5] The weld metal specimens necked, and ductile holes (holes that are elongated in the direction of the specimen axis) were observed. Similar ductile holes were noted for type 316 stainless steel base metal specimens, although the holes that formed in this case were larger than those for the weld metal. Except for the type 316 stainless steel tested at 316°C, the specimens necked considerably. The test at 316°C, although ductile, had a somewhat flatter fracture, and the holes were larger. This change at 316°C is probably a manifestation of dynamic strain aging.

Creep and Creep-Rupture Behavior

Creep-rupture tests were made on longitudinal all-weld-metal specimens taken from two pipes (Tables 5 and 6). The strength of the weld metal from the second pipe (on which the most extensive work was done) was slightly stronger than for specimens taken from the first pipe (Fig. 6).

Table 5. Creep-Rupture Properties of 16-8-2 Pipe Welds — Pipe 1

Stress (MPa)	Rupture Life (h)	Elongation (%)	Reduction of Area (%)	Minimum Creep Rate (%/h)
		Longitudinal Specimen at 566°C		
207				0.000224
241	2451.5	45.0	48.9	0.0062
276	316.7	54.5	41.3	0.0525
		Transverse Specimen at 566°C		
241	4666.3	14.1	44.7	0.00105
276	883.1	11.5	50.3	0.00535
310	272.0	10.5	39.5	0.00888
310	163.6	16.8	44.8	0.0223
345	89.3	20.3	49.0	0.0228
		Longitudinal Specimen at 649°C		
124	9208.0	42.4	59.2	0.00020
138	796.7	50.8	62.7	0.0211
155	517.9	46.3	77.2	0.0626
172	157.3	53.7	63.7	0.145
		Transverse Specimen at 649°C		
138	2917.9	18.3	35.3	0.00276
138	2938.9	23.0	57.0	0.00238
155	1135.1	19.3	55.0	0.00560
175	397.7	17.9	46.8	0.0200
172	272.5	17.9	74.4	0.0180
207	48.1	17.9	60.8	0.154

Table 6. Creep-Rupture Properties of 16-8-2 Pipe Welds — Pipe 2

Stress (MPa)	Rupture Life (h)	Elongation (%)	Reduction of Area (%)	Minimum Creep Rate (%/h)
	Longitudinal Specimen at 566°C			
241	3408.9	22.4	46.5	0.00177
259	1661.9	31.7	50.3	0.00588
276	464.6	39.6	58.3	0.0248
276	539.2	41.7	51.6	0.0226
293	294.8	35.0	47.8	0.0370
	Longitudinal Specimen at 649°C			
124				0.00019
138	2865.1	30.7	68.8	0.000585
155	1195.0	38.0	69.6	0.00455
172	266.7	41.0	71.2	0.0416
190	86.1	57.2	50.2	0.146
207	42.3	47.1	63.8	0.468

The minimum creep rate-stress relationship (Fig. 7) behaved relatively the same as the stress-rupture curves (Fig. 6): for a given stress the minimum creep rate for the second pipe weld was less than that for the first.

For comparison the rupture data were fit with the empirical relationship

$$t_R = A\sigma^{-m}\exp(Q_R/RT) \ , \tag{1}$$

and the minimum creep data were fit with

$$\dot{\varepsilon}_s = B\sigma^{n}\exp(-\ Q_c/RT) \ , \tag{2}$$

where

t_R = the rupture life in h,

$\dot{\varepsilon}_s$ = the minimum creep rate in %/h,

σ = the stress in MPa,

T = temperature in K,

A, B, m, n, Q_R, Q_c, and R = constants.

Although attempts are often made to relate Q_R and Q_c to physical processes, we will not attempt to do so in this report. These equations were used only to represent the data for discussion.

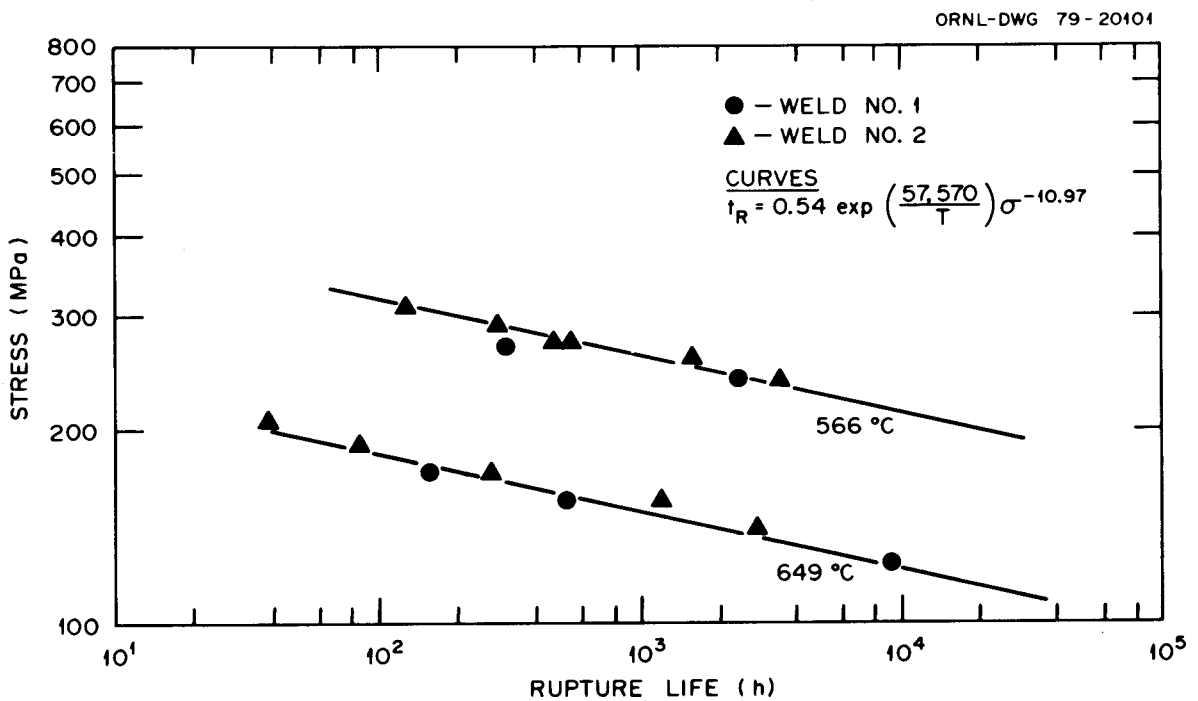

Fig. 6. Creep-Rupture Curves for 16-8-2 Pipe Welds at 566 and 649°C. Longitudinal all-weld-metal specimens were tested.

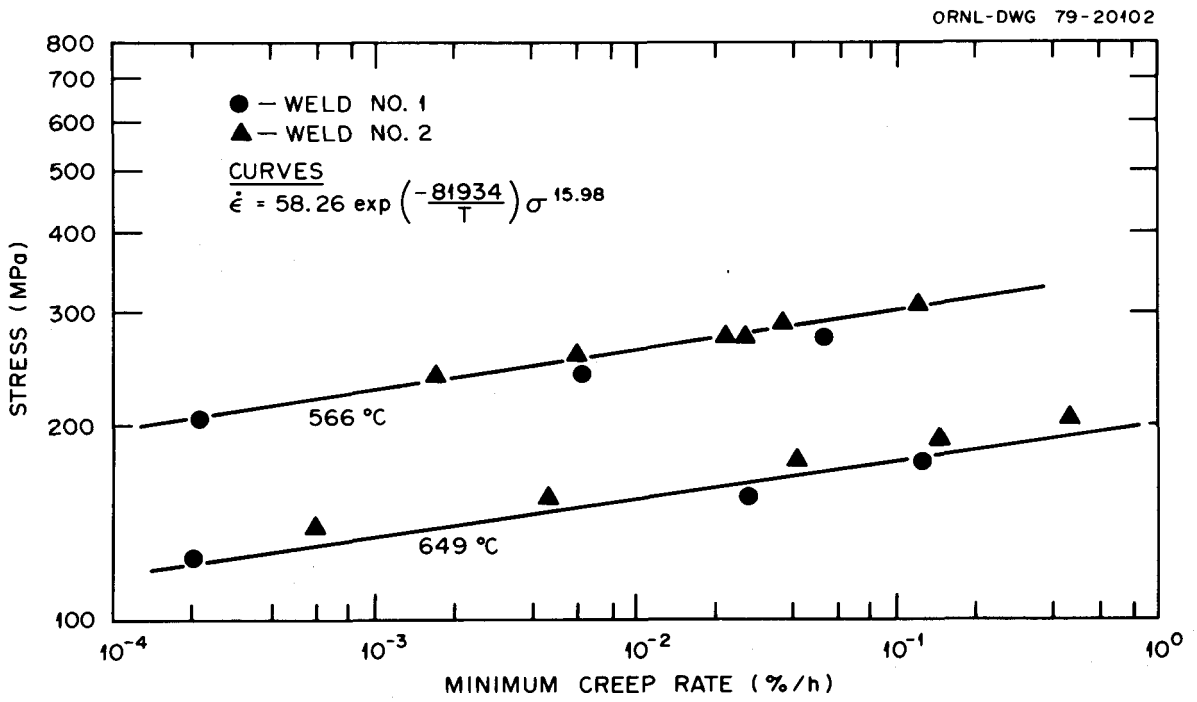

Fig. 7. Stress-Minimum Creep Rate Relationship for 16-8-2 Pipe Welds at 566 and 649°C. Longitudinal all-weld-metal specimens were tested.

The type 316 stainless steel base metal creep-rupture properties (Table 7) were determined from the three positions in the pipe: HAZ, 64 mm from the weld centerline, and 0.28 m from the weld (all are from pipe 1). In Fig. 8 the stress-rupture results for the base metal are compared with the weld metal data from Fig. 6. Although the properties varied for the specimens taken from the different positions in the pipe, the difference was not large. For the low-stress tests (long rupture times) the specimens taken 64 mm from the weld centerline were the

Table 7. Creep-Rupture Properties of Type 316 Stainless Steel Pipe

Stress (MPa)	Rupture Life (h)	Elongation (%)	Reduction of Area (%)	Minimum Creep Rate (%/h)
		Adjacent to Weld[a]		
259				0.000675
276	6209.7	33.1	38.7	0.00184
310	977.4	27.8	26.8	0.00650
345	437.2	31.1	26.2	0.010
379	177.1	33.0	30.0	0.0350
		64 mm from Weld Centerline[a]		
276	7366.0	39.8	41.0	0.00158
276	7137.8	31.2	33.3	0.00170
310	1809.0	24.6	26.3	0.0041
345	427.8	25.1	21.2	0.0165
379	206.0	29.2	28.8	0.0286
400	114.5	38.4	34.7	0.0533
		0.28 m from Weld Centerline[a]		
276	6220.2	32.6	35.9	0.00164
310	1198.7	20.4	24.2	0.00569
345	391.2	28.5	27.9	0.0100
379	183.3	32.8	27.3	0.0330
		Adjacent to Weld[b]		
158	2404.6	85.2	79.6	0.00744
172	1250.0	76.4	76.3	0.0150
207	355.7	66.0	66.0	0.054
241	87.5	57.2	61.0	0.289
		64 mm from Weld Centerline[b]		
138	3987.1	105.2	81.2	0.00385
158	2278.8	89.8	79.1	0.00950
158	2534.0	73.6	75.4	0.00663
172	1367.1	64.8	71.1	0.0104
193	647.1	63.1	72.7	0.0290
207	382.8	60.9	66.9	0.0540
227	149.6	61.8	61.8	0.157
241	72.1	69.5	60.7	0.318
		0.28 m from Weld Centerline[b]		
138	5008.2	67.7	79.1	0.00357
155	2188.4	63.9	79.9	0.00776
172	1230.4	64.1	70.6	0.0137
190	733.1	64.4	70.4	0.0240
207	317.5	62.6	63.4	0.0599
241	86.8	63.0	60.5	0.273

[a]Tested at 566°C.

[b]Tested at 649°C.

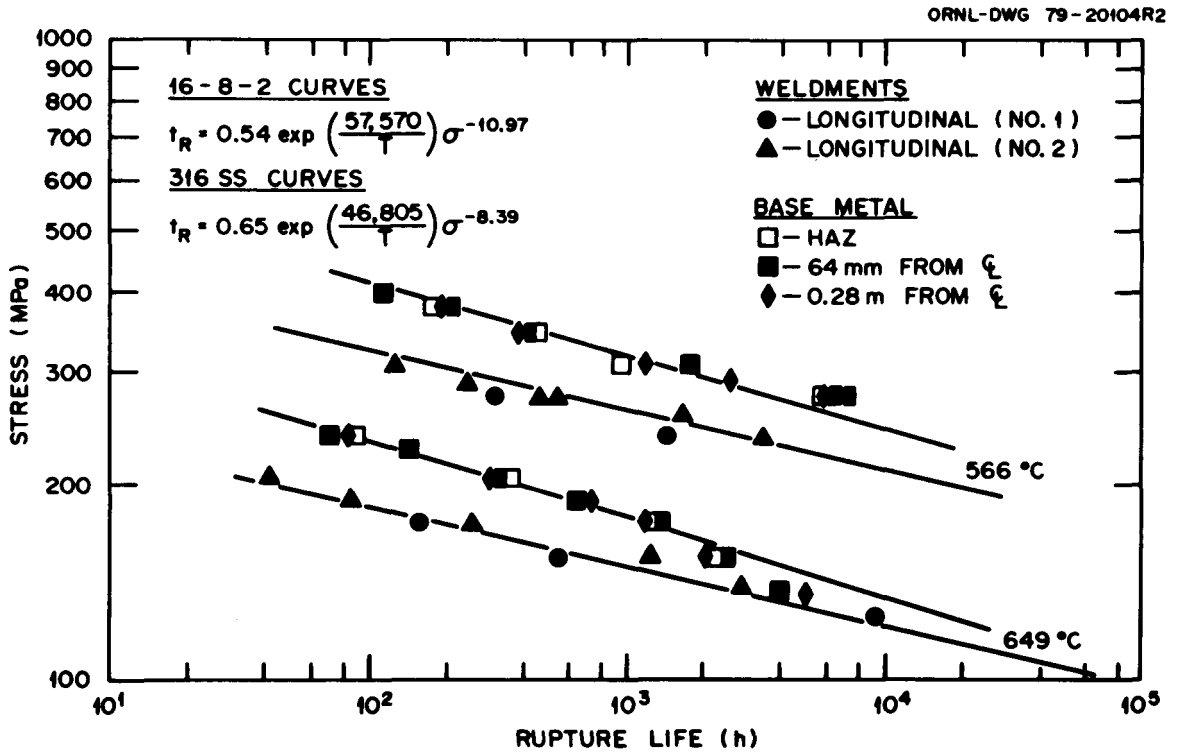

Fig. 8. A Comparison of the Creep-Rupture Behavior of the 16-8-2 Pipe Welds and the Type 316 Stainless Steel Pipe at 566 and 649°C.

strongest. The residual stresses were largest in this part of the pipe,[1] and this gave rise to a slightly larger yield strength (Fig. 4). This difference at low stresses was greatest at 566°C. For the high-stress tests (short rupture life) the rupture life for the three different types of specimens essentially did not differ.

Because of the slight strength difference, all the type 316 stainless steel data were fit with a single least squares curve and compared with the 16-8-2 longitudinal weld metal data that were similarly fit (Fig. 8).

Over the range of stresses investigated, the stress-rupture strength of the type 316 stainless steel was substantially greater than that of the weld metal. However, the slopes of the curves for the weld metal and base metal indicate that the properties approach similar values if extrapolated to longer rupture times. The same approach of properties results when the minimum creep rate data are extrapolated to lower stresses.

Although the type 316 stainless steel data were fit with straight lines in logarithmic space, curvature is indicated, especially at 649°C (Figs. 8 and 9). That is, these data could also be fit with two straight lines. More long-time tests will be required to verify this downward curvature.

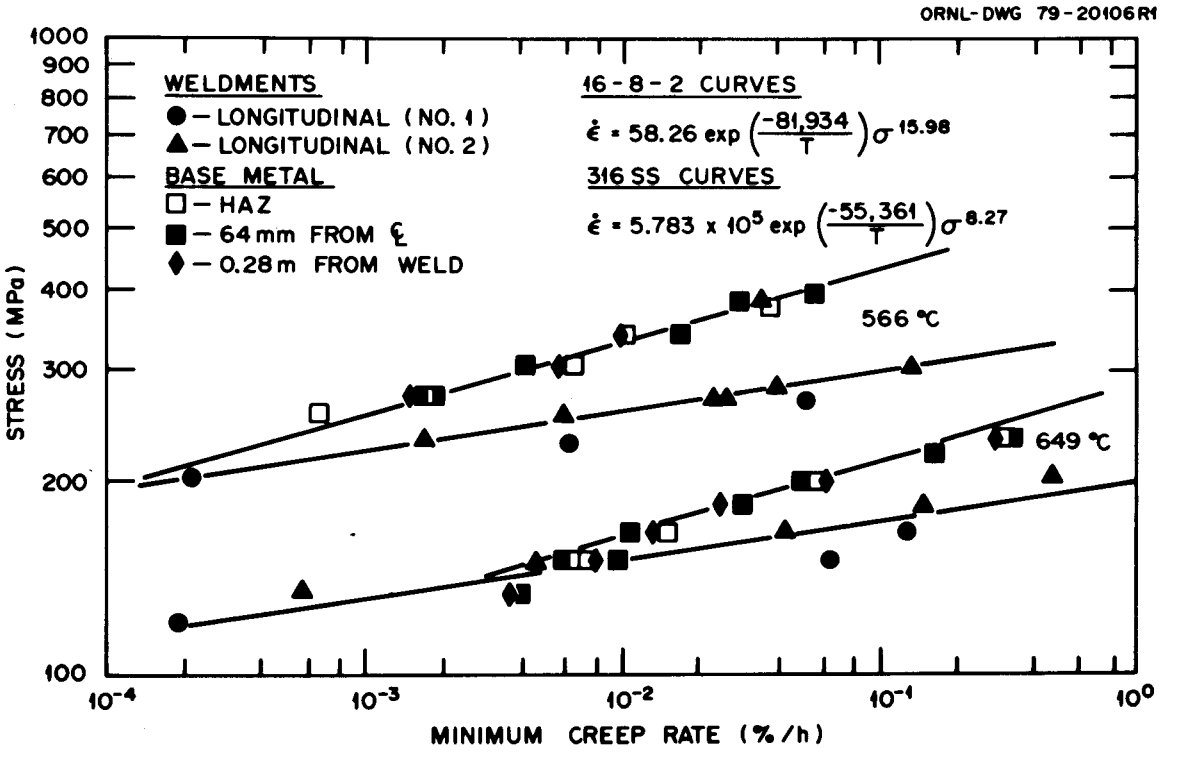

Fig. 9. A Comparison of the Minimum Creep Rate Behavior of the 16-8-2 Pipe Welds and the Type 316 Stainless Steel Pipe at 566 and 649°C.

Tests were also made on two types of composite specimens (i.e., specimens that contained both weld metal and base metal in the gage length). The first type was a transverse weldment specimen taken from across the weld that contained weld metal in the center of the gage length; weld metal made up approximately one-third of the gage length. The second type specimen was originally meant to be longitudinal all weld metal. However, the specimens were improperly machined and contained base metal in approximately 20% of the cross section of the gage length. This mistake was not discovered until several of the specimens had been tested (heat tinting during the tests revealed the machining error). Both types of composite specimens were from pipe 1.

All the transverse weldment specimens failed in the weld metal with very little deformation taking place in the base metal (there was usually less than a 5% reduction of area in the base metal). For all practical purposes it appears that these were weld metal tests on specimens with a reduced gage length.

Since the other (longitudinal) composite specimens contained only a small amount of base metal, we expected that the properties would be determined by the weld metal. Because of the apparent similarity of these composite specimens with weld metal specimens, the results were plotted with the weld metal results previously given (Fig. 10). The data from these composite specimens follow a relationship similar to that obtained for the longitudinal all-weld-metal specimens.

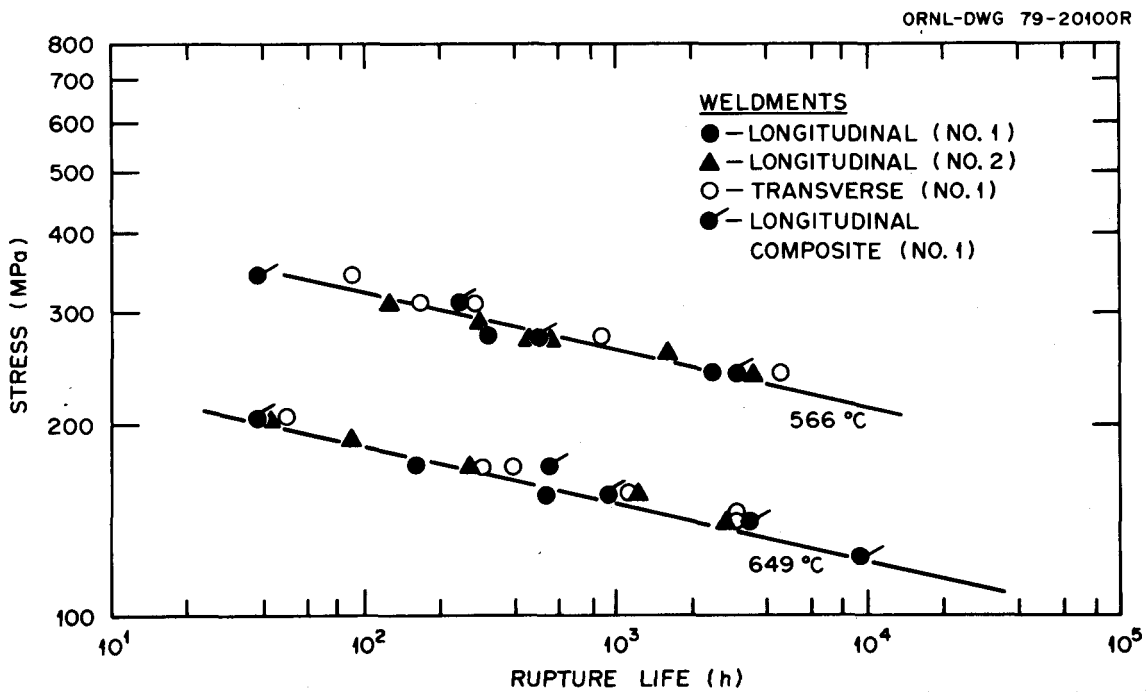

Fig. 10. Creep Rupture Properties of 16-8-2 Pipe Welds. Data are shown for longitudinal weld metal specimens, composite transverse weldment specimens, and composite longitudinal weldment specimens. The least squares curve was determined for the longitudinal all-weld-metal specimens.

The results indicate that although the failures are determined by the weld metal, the base metal properties do play a role (for the transverse weldment specimens it is not possible to separate the effect of weld metal orientation from the effect of the base metal). Both types of specimens are stronger than the all-weld-metal specimens from the same pipe. In general, the transverse weldment specimens are stronger than the other composite specimens. Note that as the stress is decreased (rupture life increases), the strength difference between the various types of specimens decreases. This difference at low stress is less at 649°C than at 566°C. Since the gage length and cross-sectional area are not easily defined for the composite specimens, no minimum creep rate comparisons are given.

Because the ductility data for the weld metal are limited, it is difficult to draw conclusions (Fig. 11). The total elongation shows a general decrease with increasing rupture life, while the reduction of area

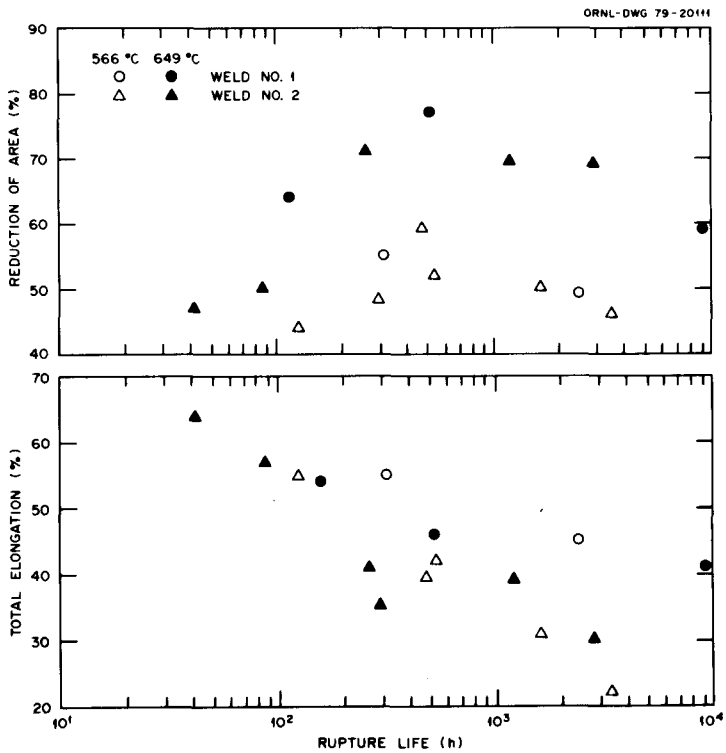

Fig. 11. Variation in Rupture Elongation and Reduction of Area with Rupture Life for 16-8-2 Longitudinal All-Weld-Metal Specimens.

shows little change. The ductility at 649°C generally exceeds that at 566°C. For the type 316 stainless steel base metal the ductility at 649°C was substantially greater than at 566°C (Fig. 12), but there was little change with rupture life. The ductilities for the type 316 stainless steel specimens taken from different positions relative to the weld did not differ substantially.

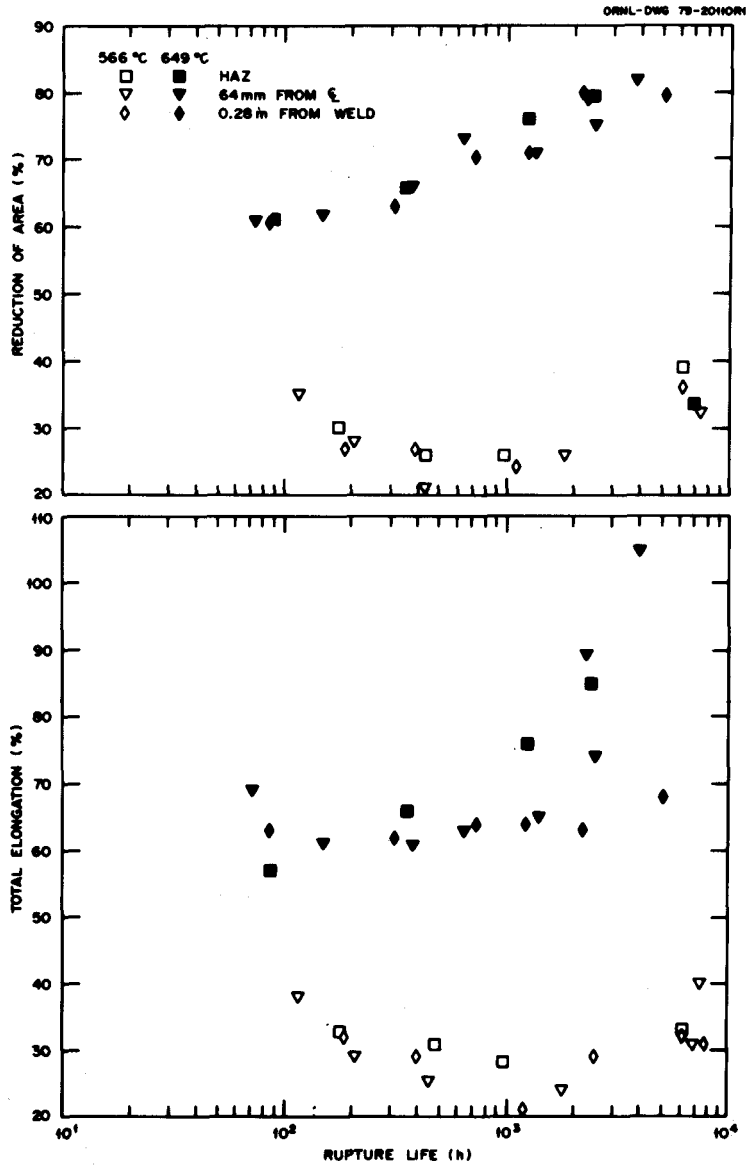

Fig. 12. Variation in Rupture Elongation and Reduction of Area with Rupture Life for Type 316 Stainless Steel Pipe.

A comparison of the reduction of area data for the weld metal and base metal (compare Figs. 11 and 12) reveals that at 566°C the weld metal has a slightly greater ductility than the type 316 stainless steel base metal over the range of stresses tested. There is less difference at 649°C, although few weld metal data exist for comparison at either temperature.

In recent years tertiary creep behavior has become important for design. The onset of tertiary creep is generally thought of as a structural instability in the material. That is, it is associated with necking or internal crack or void formation, which leads to a large increase in true stress and thus a large increase in creep rate. For many alloys the onset of tertiary creep is related to rupture life by the relation[4,6–9]

$$t_2 = A t_R^{\alpha} , \tag{3}$$

where t_2 and t_R are the times to the onset of tertiary creep and rupture, respectively, and A and α are constants. For many alloys A is independent of temperature, and α is near unity.[6–9]

To determine the onset of tertiary creep, a line was drawn parallel to the steady-state creep line that was displaced by 0.2%. The intersection of this 0.2% offset line with the creep curve was taken as the onset of tertiary creep. A logarithmic plot in accordance with Eq. (3) shows that the 16-8-2 weld metal definitely is affected by temperature (Fig. 13). The time to onset of tertiary creep is a larger fraction of the rupture life at 566°C than at 649°C. In accordance with Eq (3), the least square curves are

$$t_2 = 0.310 t_R^{1.07} \text{ (at 566°C)} , \tag{4}$$

and

$$t_2 = 0.111 t_R^{1.15} \text{ (at 649°C)} .$$

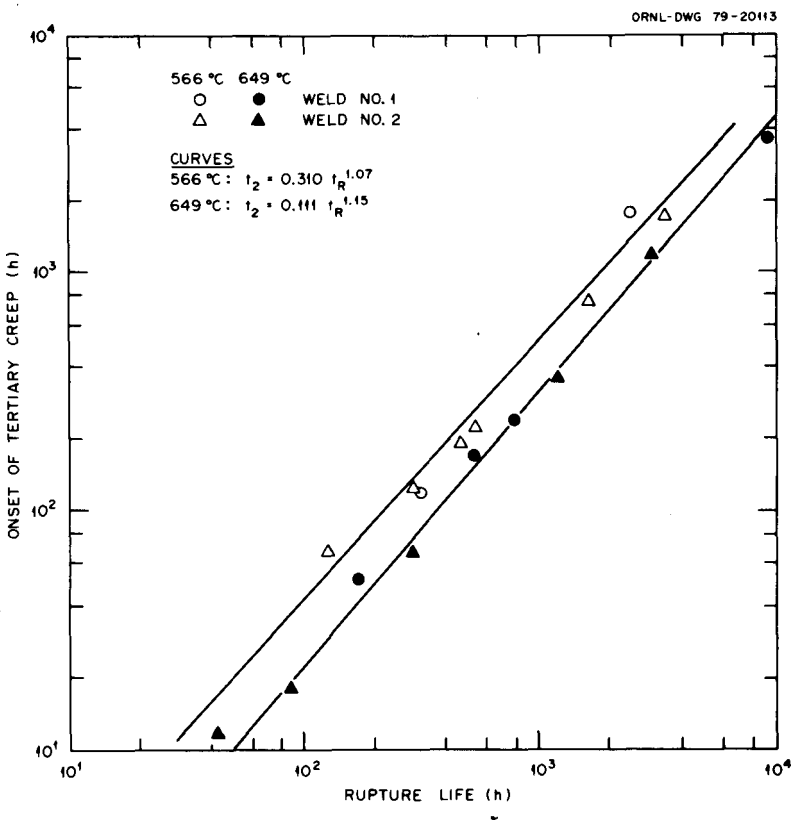

Fig. 13. Time to Onset of Tertiary Creep Plotted Against Rupture Life for 16-8-2 Pipe Welds (Longitudinal Weld Metal Tests).

The tertiary creep behavior of the type 316 stainless steel pipe is somewhat different from the behavior of the 16-8-2 weld metal (Fig. 14). At 566°C a relationship of the type given by Eq. (3) was obeyed:

$$t_2 = 0.310 t_R^{1.08} \text{ (at 566°C)} . \qquad (6)$$

This is essentially the same relationshhip as that obtained for 16-8-2 weld metal at 566°C. The 649°C data appear to follow this same relation at short times but then deviate at intermediate times. If the data are fit according to E. (1), $A \cong 1.80$ and $\alpha \cong 0.744$; these values are considerably different from those obtained in Eqs. (4) through (6) and from those obtained for most alloys,[6–9] including type 316 stainless steel.[10]

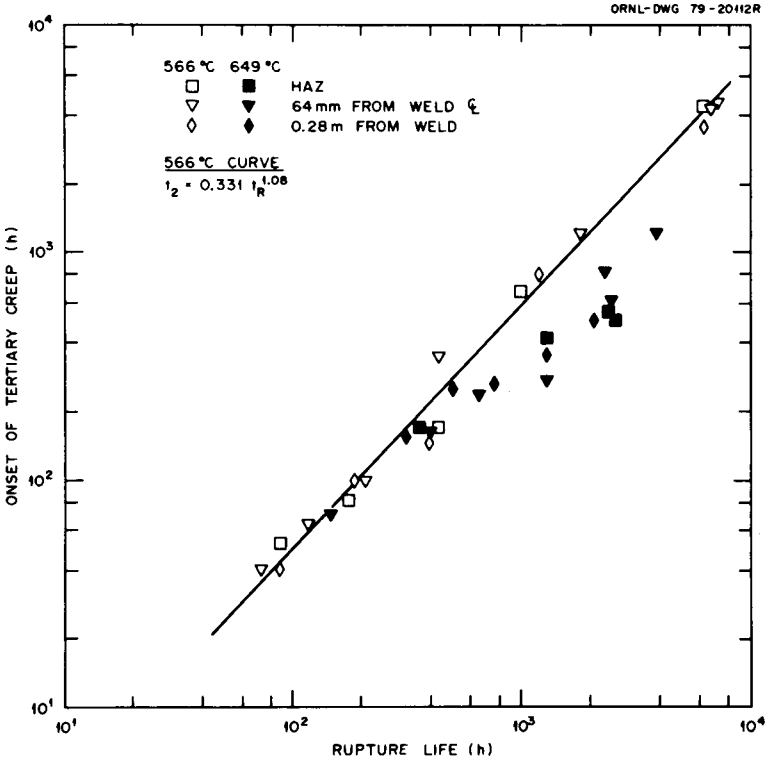

Fig. 14. Time to Onset of Tertiary Creep Plotted Against Rupture Life for Type 316 Stainless Steel Pipe Taken from Three Positions in the Pipe.

The creep strains to the onset of tertiary creep were also determined. When those data for the 16-8-2 weld metal were plotted against rupture life, the data separated according to temperature with the strain to tertiary creep at 566°C generally exceeding that at 649°C (Fig. 15). Such separation was not clear for the base metal (Fig. 16). For short rupture times the strains at 649°C exceeded those at 566°C. At longer times a crossover appears, and the tertiary strains at 566°C appear to be larger, in agreement with the weld metal data. The tertiary creep strains for the base metal exceed those for the weld metal at long times.

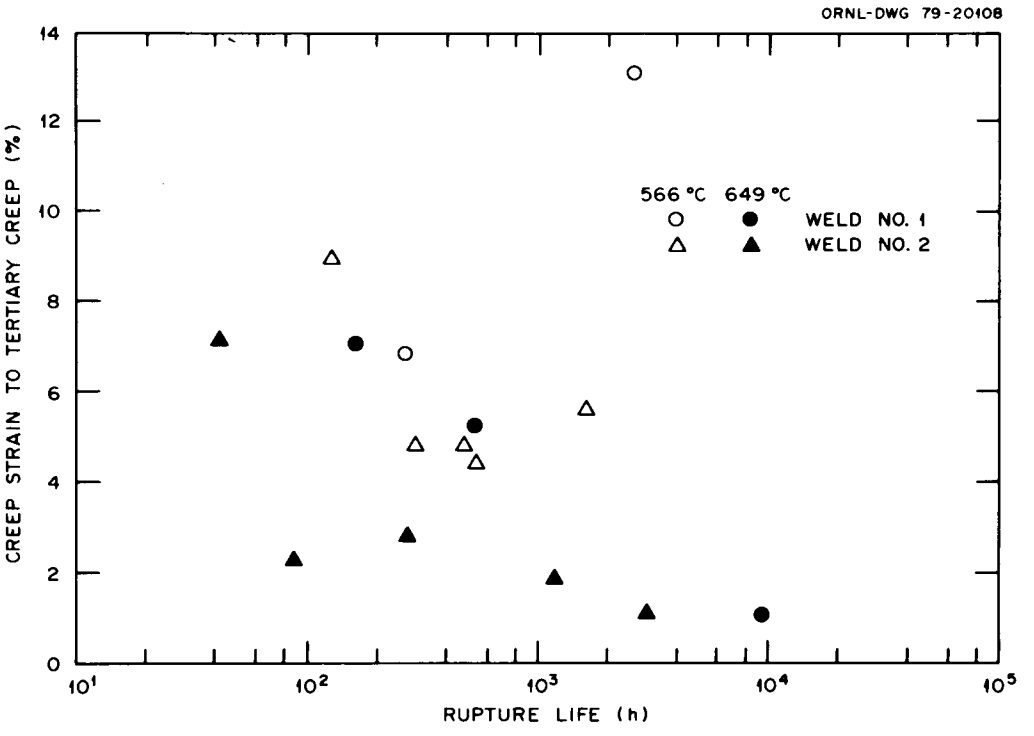

Fig. 15. Tertiary Creep Strains Plotted Against Rupture Life for 16-8-2 Pipe Welds (Longitudinal Weld Metal Tests).

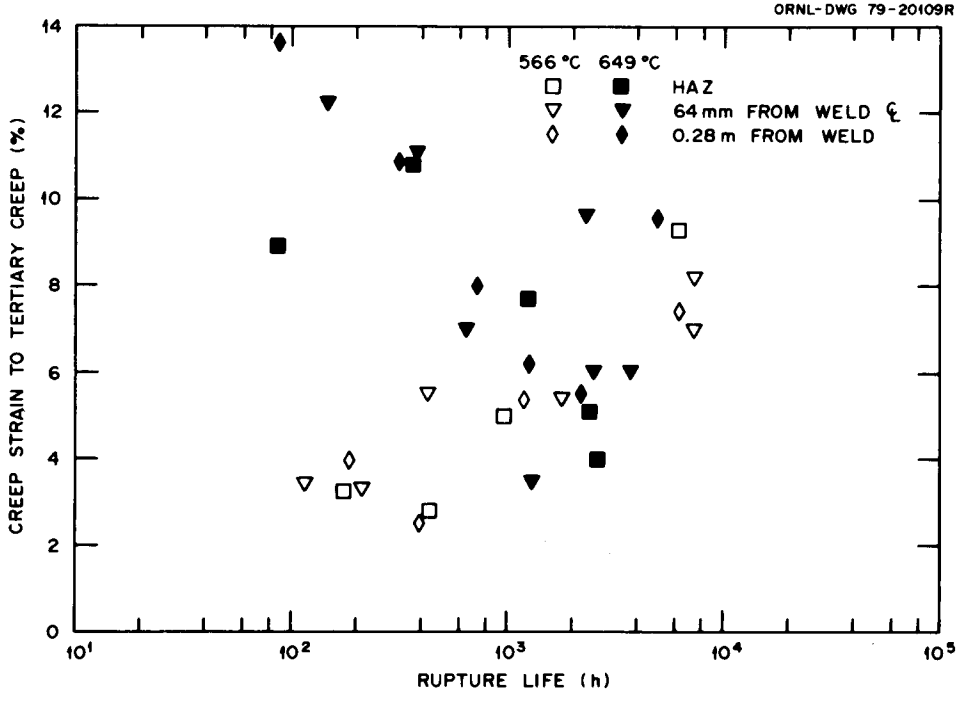

Fig. 16. Tertiary Creep Strains Plotted Against Rupture Life for Type 316 Stainless Steel Pipe Taken from Three Positions in the Pipe.

Two types of creep curves were observed: a classical curve with a primary, secondary, and tertiary creep stage and a curve that contained an essentially inverse transient stage followed by a prolonged steady-state stage (Fig. 17). When the second type of curve was observed, the end of the long steady-state stage was used to determine the onset of tertiary creep. The creep rate for this stage was also taken as the minimum creep rate, even though the inverse transient usually contained a region of steady-state creep. Classical curves occurred at 649°C, while the curves with the inverse transient stage occurred at 566°C. For the type 316

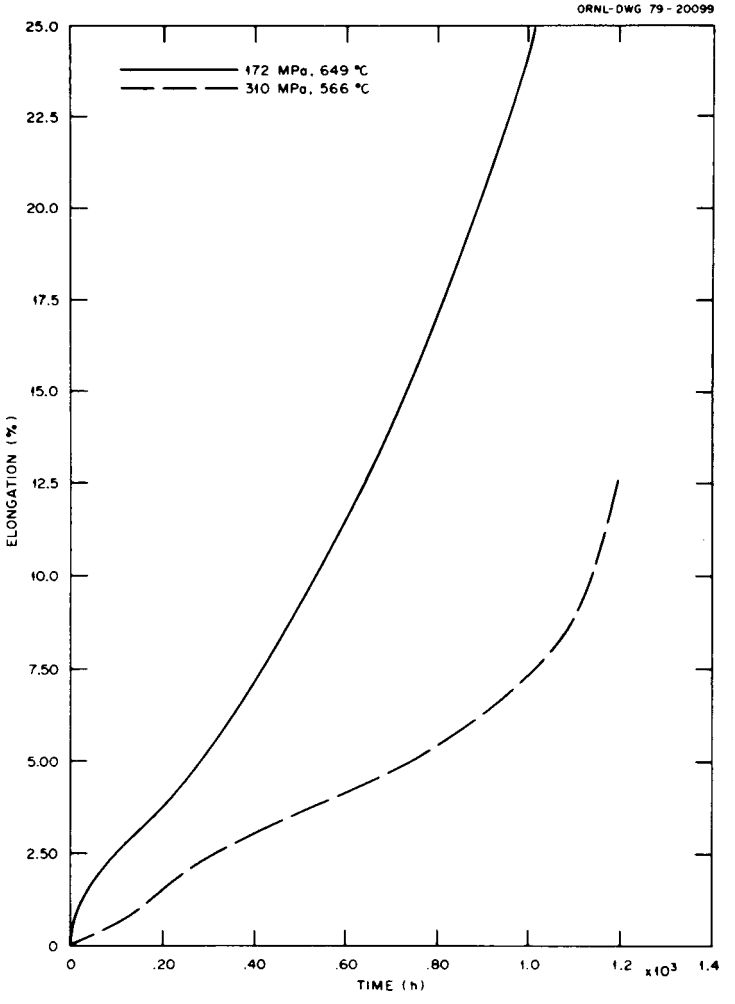

Fig. 17. Example of Different Creep Curve Shapes for Type 316 Stainless Steel Pipe Tested at 566 and 649°C. The 16-8-2 weld metal displayed a similar behavior, although the inverse transient behavior was not as pronounced at 566°C.

stainless steel base metal at 566°C, the inverse transient was easily discerned; the length of this stage decreased with increasing stress. With 16-8-2 weld metal, it was often quite difficult to detect the inverse shape, although on close examination such a curve could generally be delineated at 566°C.

The weld metal specimens necked before fracture; the fractures appeared to be a ductile-shear type. On the other hand, the type 316 stainless steel at 566°C failed with little or no necking. At 649°C fractures were more ductile and necked before fracture. The fracture mode for base metal taken from different positions in the pipe did not differ.

Metallographic examination indicated that at 566°C the weld metal specimen tested at 310 MPa contained the start of w-type crack formation. The specimen tested at 241 MPa had extensive cracking along the gage length, although the cracking was almost exclusively confined to only one of the three weld passes that were in the specimen cross section (Fig. 18).

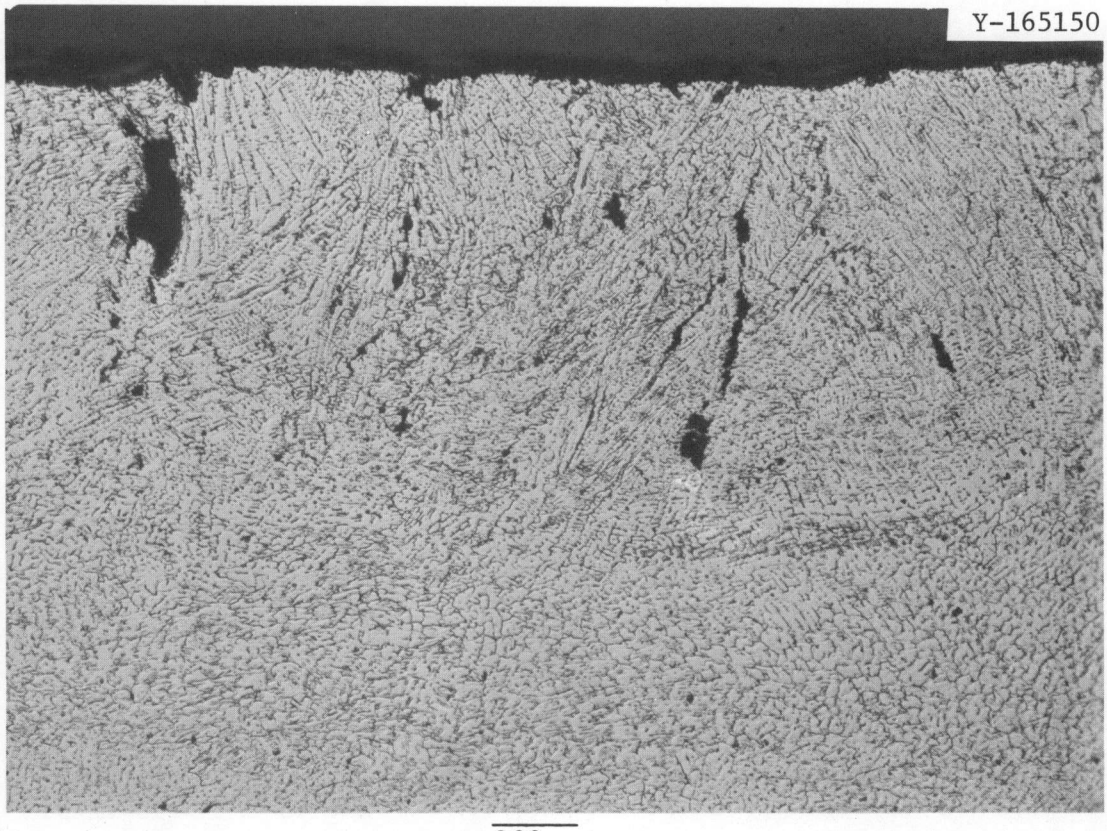

Fig. 18. Intersubstructural Cracks in 16-8-2 Weld Metal Specimen Tested at 241 MPa at 566°C. Etched with aqua regia.

For specimens examined at 649°C, only the weld metal specimen tested at the lowest stress (124 MPa) showed any indication of void or crack formation. There were only a few such defects, and the failure was quite ductile.

The longitudinal composite specimen tested at 649°C at 124 MPa (Fig. 19) showed that the most extensive void and crack formation occurred in the HAZ. The HAZ of the type 316 stainless steel had extensive grain growth occurring during the welding process. Furthermore, large grain boundary cracks occurred in the grain growth regions. Also, many small grain boundary voids were visible in the base metal. Very few voids or

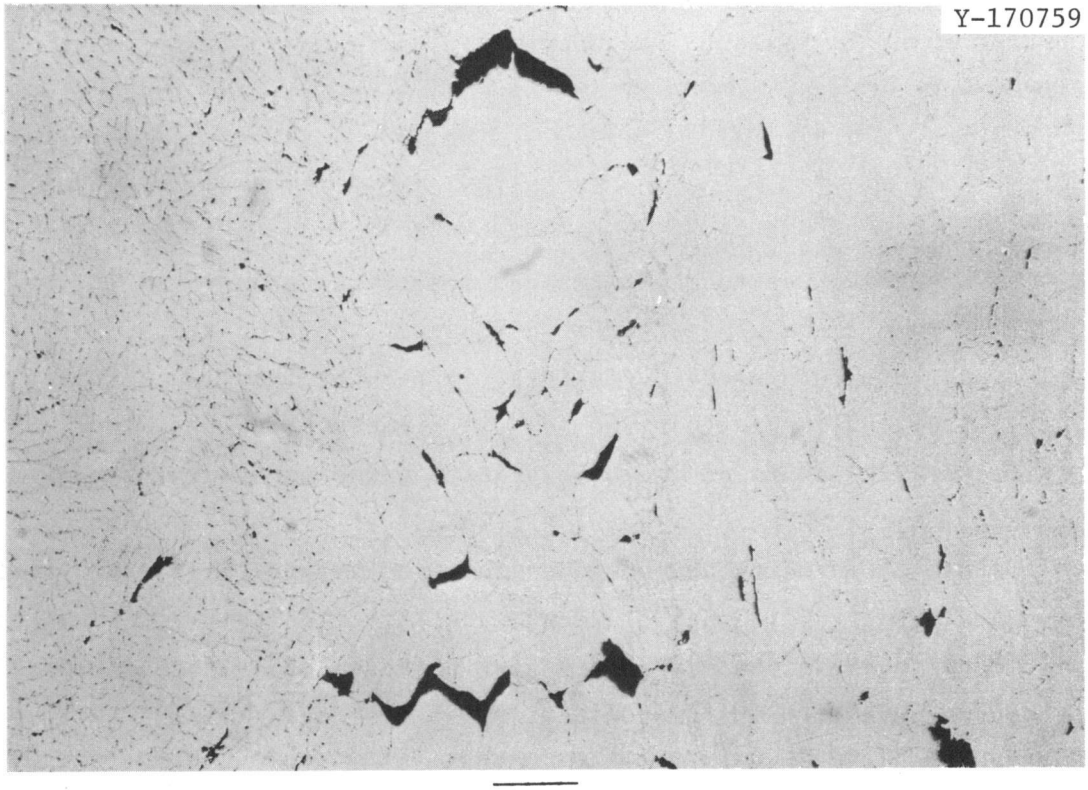

Fig. 19. Microstructure of Longitudinal, Composite Specimen That Was Tested at 124 MPa at 649°C and Subsequently Ruptured After 9264 h. The extensive cracking shown in the center of the photomicrograph has occurred in the heat-affected zone. Less extensive void and crack formation occurred in the base metal (right side) and still less in the weld metal (left side). Etched with a heated solution of 15 g $KFe(CN)_6$, 15 g KOH, and 100 mL H_2O.

cracks were visible in the weld metal, and these were adjacent to the HAZ. The fracture mode of the weld metal and base metal portion of the fracture surface appeared quite ductile (transgranular), while the HAZ fracture appeared intergranular.

The type 316 stainless steel base metal specimens showed distinctly different behavior at 566 and 649°C. The behavior was also different from the weld metal tests. At 566°C the fractures were quite flat with little or no neck formation. All the specimens formed wedge-type cracks within grain boundaries [Fig. 20(a)]. The extent of this type cracking increased with decreasing stress. At 649°C the fractures appeared much more ductile and were accompanied by necking [Fig. 20(b)]. The holes that formed in the gage length were indicative of a ductile failure (holes that were elongated along the axis of the specimen); there were few indications of w-type cracks.

DISCUSSION

Our objective was to determine the mechanical properties of the pipe weld to compare these properties with those of the type 316 stainless steel pipe. Steichen[3] previously investigated the base metal properties for similar pipes fabricated from several different heats of type 316 stainless steel. Included in those studies was a limited number of tests on heat 55318, the heat of type 316 stainless steel pipe used in this study. From those tests he concluded that the properties varied little from heat to heat. Although Steichen made a few tests on specimens taken from the cylindrical orientation (the orientation of specimens tested in this study), most of his tests were from specimens taken in the axial direction.

In this study we chose to test type 316 stainless steel specimens from the cylindrical direction (parallel to the pipe weld) because we wished to determine the effect of welding on the type 316 stainless steel. Thus, cylindrical specimens were taken from the HAZ and from the position of maximum residual stress; specimens from these two positions were then compared with cylindrical specimens taken from the position where the material was unaffected by welding, 0.28 m from the weld.

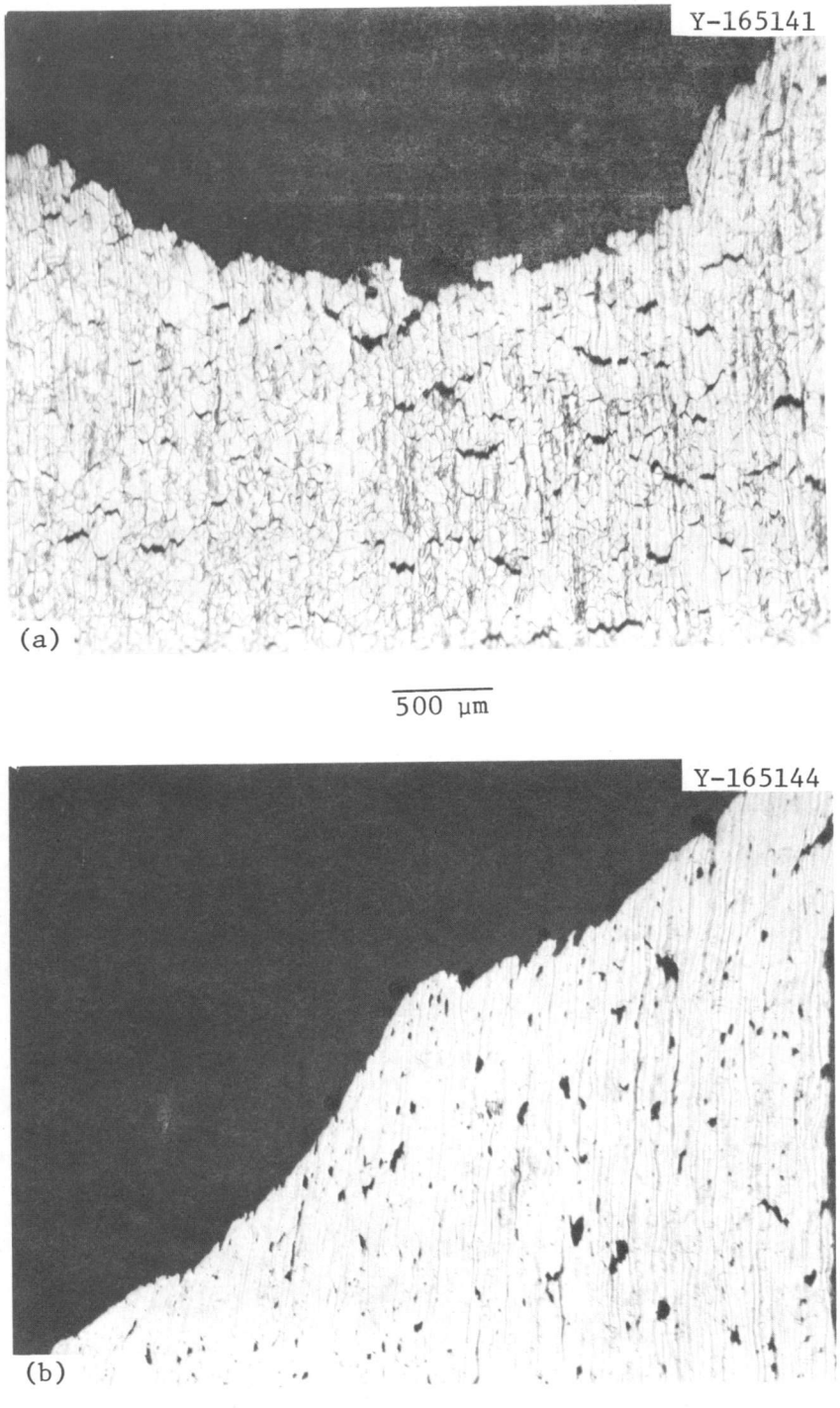

Fig. 20. Fracture Morphologies of Type 316 Stainless Steel Pipe Taken 0.28 m from the Weld and Tested at (a) 310 MPa at 566°C and (b) 172 MPa at 649°C. Intergranular separation occurred at 566°C, while highly ductile fractures were observed at 649°C. Etched with aqua regia.

The tensile data collected in this study confirmed Steichen's conclusion that specimen orientation (relative to the pipe) does not significantly affect the strength.[3] The YS and UTS values of the HAZ and the steel 0.28 m from the weld were essentially the same and agreed very well with those determined by Steichen; they were slightly less (about 10%) than the average of the Steichen values.

Our tensile studies on the base metal indicate that the major effect of welding was caused by the residual stresses. However, only the YS was affected.

The 16-8-2 weld metal tensile behavior relative to the type 316 stainless steel base metal was similar to results of other studies, which showed that between 25 and 649°C the YS of the weld metal was considerably greater than that of type 316 stainless steel base metal (unaffected by welding), while the UTS above 25°C fell considerably below that of the base metal. When compared with the average and minimum type 316 stainless steel base metal properties given by Smith,[2] the 16-8-2 pipe welds had UTS values comparable to the minimum values up to 566°C. The values at 649°C fell significantly below the minimum (Fig. 3). The YS values for the 16-8-2 pipe welds were significantly above those of the average base metal properties over the entire temperature range (Fig. 3).

Steichen[3] also determined creep-rupture properties. Although most of his tests were on heat 55320, several tests were made on the heat of pipe used for this study (55318). Again, he studied mostly axial specimens, with a few tests on cylindrical specimens for comparison. In Fig. 21 the log-log straight lines from Steichen's creep-rupture results are shown along with the data obtained in this study. Agreement is excellent. Similar agreement resulted when minimum creep rate data were compared (Fig. 22).

The only apparent divergence in the creep-rupture curves occurs at 649°C, where all the data fall on Steichen's curve except the long-time tests (Fig. 21). These fall below Steichen's curve. Steichen's longest test (one test at 165 MPa that ruptured after 2132 h) has no indication of a break in the creep-rupture curve as these results would indicate. The

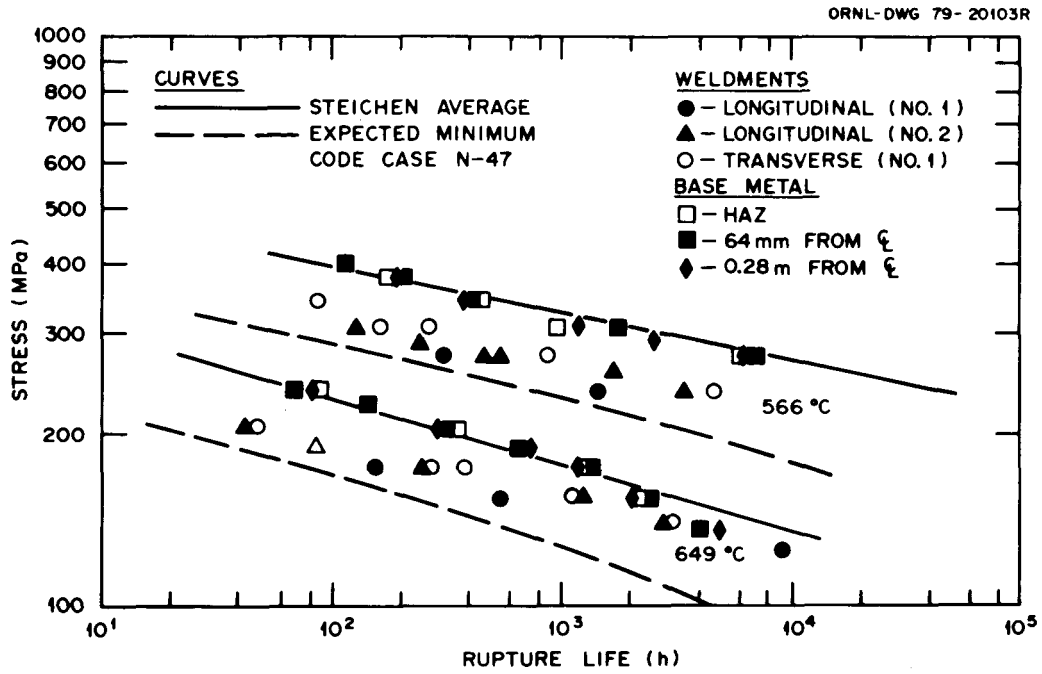

Fig. 21. A Comparison of the 16-8-2 Pipe Weld and the Type 316 Stainless Steel Pipe Creep-Rupture Data with the Expected Minimum for Type 316 Stainless Steel Given in Code Case N-47. Also shown are type 316 stainless pipe data from Steichen (HEDL-TME 75-15).

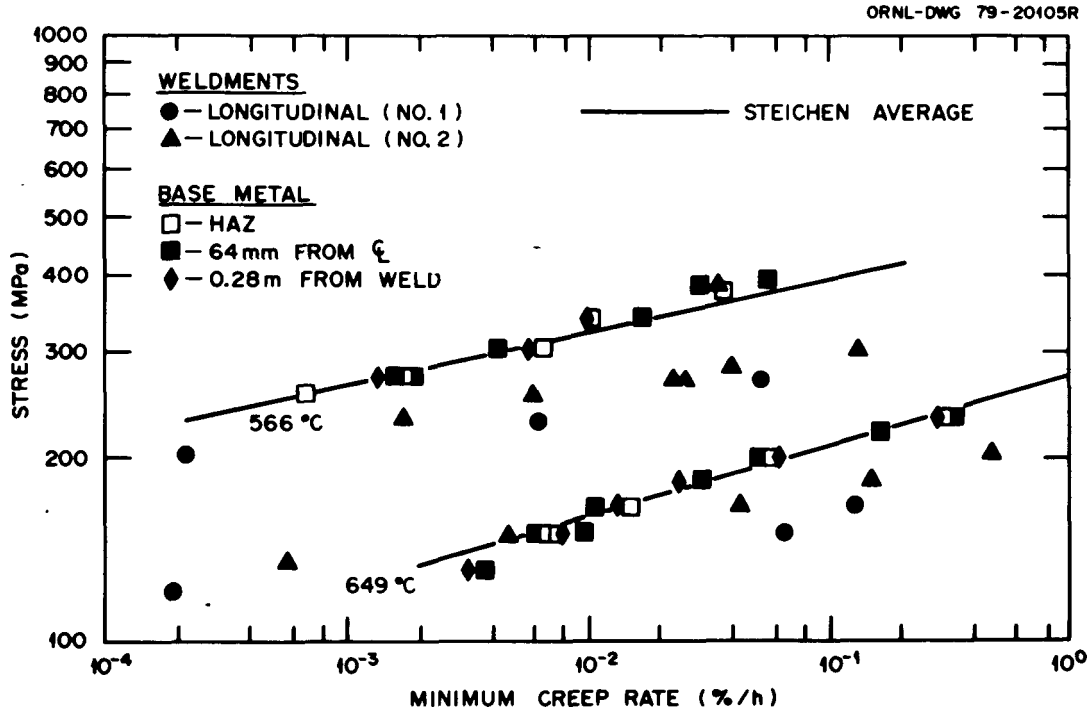

Fig. 22. A Comparison of the Stress-Minimum Creep Rate Data for the Type 316 Stainless Steel Pipe with the Average Curve Obtained by Steichen (HEDL-TME 75-15) on Similar Pipe.

possibility of downward curvature in the creep-rupture (Fig. 8) and minimum creep rate data (Fig. 9) was pointed out in the previous section. In the future we intend to get more long-time data to verify that these curves do contain such a break.

The comparison between the creep-rupture properties of 16-8-2 weld metal and type 316 stainless steel base metal is most interesting. Although the type 316 stainless steel is definitely superior at high stresses, the difference in slopes for the creep-rupture (Fig. 8) and the minimum creep rate curves (Fig. 9) for these two steels indicates that the difference in properties becomes less for long-time tests. The approach of properties is more pronounced at 649°C than at 566°C.

We also compared our 16-8-2 pipe weld data with the minimum expected rupture curves given in the *American Society of Mechanical Engineers (ASME) Boiler and Pressure Vessel Code*, Case N-47. At both temperatures the expected minimum falls well below the data for the pipe welds (Fig. 21). Previously, we reported on the properties of several large 16-8-2 weldments made by the submerged-arc process.[4] Those welds had creep-rupture properties similar to or below those of the Code Case N-47 expected minimum. Thus, the pipe welds made by the gas tungsten-arc process are considerably stronger than the submerged-arc welds.

The main difference in chemical composition between type 316 stainless steel and 16-8-2 weld wire is in the nickel (Table 1). Type 316 stainless steel has about 13.5 vs 8.6 wt % Ni for the 16-8-2; because of the dilution during welding, this difference is somewhat less for the weld metal deposit. Nickel has a minor effect on the solid-solution or dispersion-hardening processes in an austenitic stainless steel;[11] however, lowering the nickel content promotes ferrite formation during solidification, which can affect the strength. Thus, the tensile and creep property differences between 16-8-2 and type 316 stainless steel must mainly reflect microstructural differences in the weld metal (Fig. 2) and in the base metal (Fig. 3).

Correlations have been developed to predict the room temperature strengths of austenitic stainless steels from the chemical composition and microstructural features.[11] In these equations the YS and UTS values are

expressed as functions of C, Si, N, Cr, Ni, Mo, V, W, Nb, Ti, Al, and δ-ferrite content, grain size, and twin spacing. Assuming that nickel content is the only compositional difference between 16-8-2 and type 316 stainless steel, we used these equations[11] to try to understand the difference in these properties for the two materials. By subtracting the correlation for the 16-8-2 weld metal (subscript *WM*) from the correlation for the base metal (subscript *BM*) we obtained

$$Y_{BM} - Y_{WM} = 15.4\left[0.46\left(d_{BM}^{-1/2} - d_{WM}^{-1/2}\right) - 0.16(\sigma\text{-ferrite})_{WM}\right], \qquad (7)$$

and

$$U_{BM} - U_{WM} = 15.4\left\{0.11\left[(\%\ \text{Ni})_{BM} - (\%\ \text{Ni})_{WM}\right] - 0.14(\sigma\text{-ferrite})_{WM} + 0.82t_{BM}^{-1/2}\right\}, \qquad (8)$$

where

Y = the yield strength in MPa,

d = the grain diameter in mm,

U = the ultimate tensile strength in MPa,

t = the twin spacing in mm.

It is not possible to derive absolute values from these equations since it is not possible to get an accurate measure for d_{WM}. Because the weld metal is substructurally complex, the microstructural feature for which d_{WM} should account is not immediately obvious (i.e., grain structure or dendrite structure). Nevertheless, qualitatively these equations allow us to conclude that the YS advantage of the 16-8-2 weld metal over the type 316 stainless steel pipe (except that taken 64 mm from the weld) must arise from differences in grain size — whatever the proper measure may be — and possibly from the δ-ferrite content, although it is difficult to see how such a small amount could have a large effect. The extra strength of the pipe taken 64 mm from the weld could be explained by the effects of cold work during welding (residual stresses). At room temperature, where these equations apply, the UTS values of the two

materials essentially do not differ (Fig. 3). Thus, the strengthening by the δ-ferrite in the 16-8-2 weld metal must offset the differences in nickel content and twin spacing that would favor the type 316 stainless steel.

The differences in elevated-temperature strength are more complicated. For creep tests, dispersion strengthening resulting from carbides becomes important (the large δ-ferrite particles probably have little effect on the creep properties). The convergence of creep-rupture properties (Figs. 8 and 9) could possibly reflect the variance in the precipitation kinetics resulting from differences in the original microstructure of the two product forms. In the weld metal the liquid is cooled rather quickly, thus inhibiting precipitation. On the other hand, during processing of the pipe, precipitation is promoted. This becomes somewhat evident when the longitudinal composite specimen that was tested for over 9000 h at 649°C is examined (Fig. 23). Matrix precipitate particles are easily resolved in the base metal [Fig. 23(a)] and in the HAZ [Fig. 23(b)], but not in the weld metal [Fig. 23(c)]. This could indicate that overaged precipitate particles exist for the base metal and HAZ, while fine precipitate particles are forming in the matrix of the weld metal. Thus, time is required at the creep test temperature for precipitation strengthening processes in the 16-8-2 to develop to the same point as they had in the pipe during fabrication. If this is the case, the apparent approach of properties might be expected. The more rapid approach at 649°C is also expected since precipitation is a thermally activated process. If overaging becomes important a crossover, of properties at longer test times may well occur, as appears to be happening in the minimum creep rate data at 649°C (Fig. 9).

With a selective etching technique we were able to identify sigma phase in the 16-8-2 weld metal of creep specimens that had been exposed to 566 or 649°C for several-thousand hours. The sigma phase had formed from the δ-ferrite particles that outlined the cellular dendritic structure. Because only 2 to 3% δ-ferrite was in the weld metal, only a small amount of sigma phase was formed. This small amount of sigma did not appear to affect the creep fracture process.

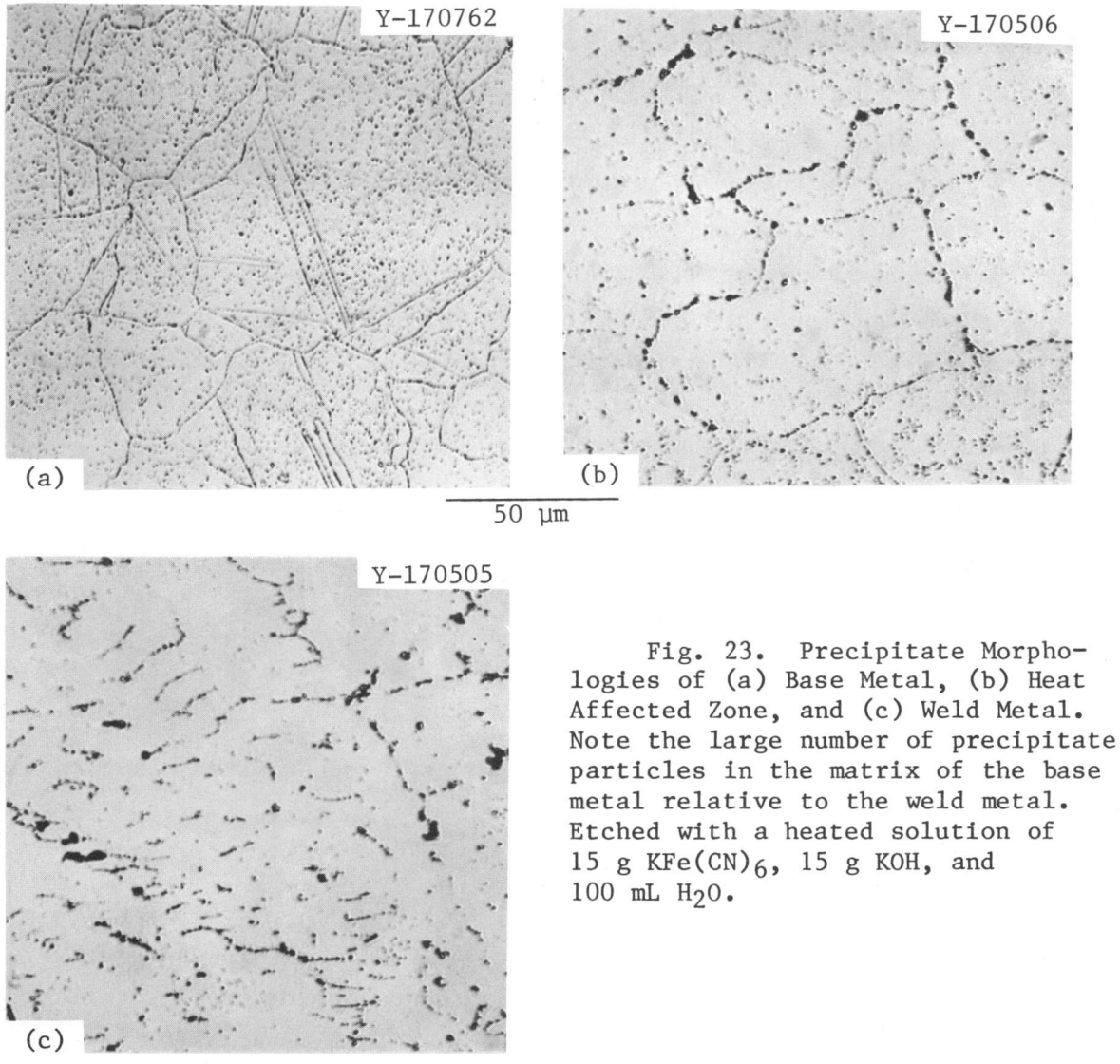

Fig. 23. Precipitate Morphologies of (a) Base Metal, (b) Heat Affected Zone, and (c) Weld Metal. Note the large number of precipitate particles in the matrix of the base metal relative to the weld metal. Etched with a heated solution of 15 g $KFe(CN)_6$, 15 g KOH, and 100 mL H_2O.

The unusual tertiary creep behavior for the type 316 stainless steel pipe (Fig. 14) is somewhat similar to that observed by Swindeman in type 304 stainless steel.[12] He found that Eq. (3) with $\alpha = 1$ was obeyed at $t \gtrsim 704°C$ (tests were at 704, 760, 816, and 871°C). For short- and long-term tests at 649°C, Eq. (3) was also obeyed. At intermediate times, however, a pronounced deviation occurred in the same direction as the 649°C data of this study (Fig. 14). Similar deviations were observed at 621 and 593°C, although the extent of the deviations decreased with decreasing temperature. At 566°C the data again obeyed Eq. (3).

The behavior of the type 316 stainless steel pipe appears to be similar to that observed for the type 304 stainless steel. Like Swindeman's results, Eq. (3) is followed at 566°C and not at 649°C. For type 316 stainless steel pipe (Fig. 14), a convergence of properties similar to that noted by Swindeman at long times is not obvious; perhaps the long-time tests presently in progress will show that such convergence of properties also occurs for the type 316 stainless steel pipe.

It is interesting to note that at 566°C the correlations for tertiary creep for the type 316 stainless steel pipe [Eq. (6)] and 16-8-2 weld metal [Eq. (4)] are essentially the same. The deviation of the 649°C data from Eq. (4) for the 16-8-2 weld metal (Fig. 13) is in the same direction as the deviation at intermediate times for the type 316 stainless steel pipe from Eq. (6) (Fig. 14). The major difference is that the 16-8-2 data at 649°C do not approach the 566°C curve at short times. This may indicate that the cause of the deviation has similar origins in the two materials.

Swindeman was not able to explain the deviation from Eq. (3) in type 304 stainless steel.[12] Similar deviations in other materials have been attributed to metallurgical instabilities.[9] The inverse transient creep behavior (Fig. 17) is a manifestation of a metallurgical instability. As stated above, the convergence of the creep and creep-rupture properties at long times at 649°C may be the result of metallurgical instabilities (carbide precipitation). To determine the nature of these metallurgical instabilities and to discover whether all the observations attributed to metallurgical instabilities are related to the same metallurgical reactions were beyond the scope of this work.

SUMMARY AND CONCLUSIONS

Tensile, creep, and creep-rupture properties were determined for 16-8-2 girth welds that were made on 0.71-m-diam type 316 stainless steel seamless pipe with a 9.5-mm-thick wall. The welds were made with the automatic gas tungsten-arc process, using cold-wire filler additions. Tests were also made on the type 316 stainless steel pipe taken from

three different pipe positions (relative to the weld): at a position immediately adjacent to the weld (HAZ), at the position of maximum residual stress caused by welding (64 mm from the weld centerline), and at a position well removed from the weld (0.28 m away) where welding does not affect the properties. The following summarizes the results and conclusions:

1. The YS of the type 316 stainless steel pipe over the range 25 to 649°C was increased considerably by the residual stress of welding. The YS values of the steel from the HAZ and from a position that was unaffected by welding did not differ. Furthermore, the UTS values of the type 316 stainless steel from the three different positions in the pipe did not differ.

2. From 25 to 649°C the YS of the 16-8-2 weld metal was up to 60% larger than the values for the type 316 stainless steel from the HAZ and for the area unaffected by welding. It was similar to the YS of the steel taken from the position of maximum residual stress.

3. At room temperature the UTS of the 16-8-2 weld metal was similar to that for the type 316 stainless steel. Above room temperature it was up to 20% less than that of the type 316 stainless steel.

4. The YS of the 16-8-2 weld metal from 25 to 649°C was well above the average for type 316 stainless steel; the UTS of the 16-8-2 weld metal was near the minimum for type 316 stainless steel except at room temperature, where it was above average.

5. Up to several-thousand hours the creep-rupture curves for the 16-8-2 weld metal at 566 and 649°C fell well below those for the type 316 stainless steel. However, a convergence of properties at long rupture times was indicated. This was much more pronounced in the stress-minimum creep rate relationships, especially at 649°C.

6. A relationship between the time to the onset of tertiary creep and rupture life was sought. The 16-8-2 weld metal and the type 316 stainless steel pipe behaved differently.

ACKNOWLEDGMENTS

We thank the following people for helping to complete this work: E. Bolling carried out the experimental work; C. W. Houck performed the metallography; T. E. Hebble fit the data to empirical relationships; S. A. David, J. P. Strizak, C. R. Brinkman, and G. M. Slaughter reviewed the manuscript; B. G. Ashdown edited the manuscript; and K. A. Witherspoon prepared the report for final publication.

REFERENCES

1. L. Adler, K. V. Cook, B. R. Dewey, and R. T. King, "The Relationship Between Ultrasonic Rayleigh Waves and Surface Residual Stress," *Mater. Eval.* 35(7): 93–96 (1977).
2. G. V. Smith, *An Evaluation of the Yield, Tensile, Creep and Rupture Strengths of Wrought 304, 316, 321, and 347 Stainless Steels at Elevated Temperatures*, *ASTM Data Ser.* DS 5 S2, American Society for Testing and Materials, Philadelphia, February 1969.
3. J. M. Steichen, *Mechanical Properties of FFTF Primary Outlet Piping*, HEDL-TME-75-15 (January 1975).
4. R. L. Klueh and D. P. Edmonds, *Effect of Flux Type on Elevated-Temperature Strength of 16-8-2 Submerged-Arc Welds*, ORNL-5594 (February 1980).
5. R. L. Klueh and J. F. King, *Elevated-Temperature Tensile Properties of ERNiCr-3 Weld Metal*, ORNL-5354 (December 1977).
6. F. Garofalo et al., "Creep and Creep-Rupture Relationships in an Austenitic Stainless Steel," *Trans. Am. Inst. Min. Metall. Pet. Eng.* 221: 310–19 (1961).
7. W. E. Leyda and J. P. Rowe, *A Study of Time for Departure from Secondary Creep for Eighteen Steels, ASM Tech. Rep.* P9-6.1, American Society for Metals, Metals Park, Ohio, 1969.
8. M. K. Booker and V. K. Sikka, *Interrelationships Between Creep Life Criteria for Four Nuclear Structural Materials*, ORNL/TM-4997 (August 1975).

9. R. L. Klueh, "The Tertiary Creep Behavior of Annealed 2 1/4 Cr-1 Mo Steel," *J. Nucl. Mater.* 79: 363–71 (1979).

10. M. K. Booker and V. K. Sikka, "A Study of Tertiary Creep Instability in Several Elevated-Temperature Structural Materials," pp. 129–48 in *Ductility and Toughness Considerations in Elevated-Temperature Service*, American Society of Mechanical Engineers, New York, 1978.

11. F. B. Pickering, *Physical Metallurgy and the Design of Steels*, Applied Science Publishers, London, 1978.

12. R. W. Swindeman, *Analysis of Creep-Rupture Data for Reference Heat of Type 304 Stainless Steel (25-mm Plate)*, ORNL-5565 (September 1979).

Blank Page

ORNL-5660
Distribution
Categories
UC-79h, -k, -r

INTERNAL DISTRIBUTION

1–2. Central Research Library
3. Document Reference Section
4–5. Laboratory Records Department
6. Laboratory Records, ORNL RC
7. ORNL Patent Section
8. J. J. Blass
9. M. K. Booker
10. C. R. Brinkman
11. J. M. Corum
12. J. H. DeVan
13–22. D. P. Edmonds
23. G. F. Flanagan
24–26. M. R. Hill
27. R. L. Huddleston
28. J. F. King
29–33. R. L. Klueh
34. W. J. McAffee
35. J. W. McEnerney
36. C. E. Pugh
37. V. K. Sikka
38. G. M. Slaughter
39. J. H. Smith
40. R. W. Swindman
41. G. T. Yahr
42. A. L. Bement, Jr. (Consultant)
43. E. H. Kottcamp, Jr. (Consultant)
44. Alan Lawley (Consultant)
45. T. B. Massalski (Consultant)
46. M. J. Mayfield (Consultant)
47. R. H. Redwine (Consultant)
48. J. T. Stringer (Consultant)

EXTERNAL DISTRIBUTION

49–50. DOE, DIVISION OF REACTOR AND TECHNOLOGY, Washington, DC 20545
Director

51. DOE, OAK RIDGE OPERATIONS OFFICE, P.O. Box E, Oak Ridge, TN 37830
Office of Assistant Manager for Energy Research and Development

52-253. DOE, TECHNICAL INFORMATION CENTER, P.O. Box 62, Oak Ridge, TN 37830
For distribution as shown in TID-4500 Distribution Category, UC-79h (Structural Materials and Design Engineering); UC-79k (Components); and UC-79r (Structural and Component Materials Development)

☆U.S. GOVERNMENT PRINTING OFFICE: 1980-640-245/236